Inorganic Chemistry

Article

pubs.acs.org/IC

Quantitative Assessment of Halogen Bonding Utilizing Vibrational Spectroscopy

Vytor Oliveira, Elfi Kraka,* and Dieter Cremer*

Computational and Theoretical Chemistry Group, Department of Chemistry, Southern Methodist University (SMU), 3215 Daniel Avenue, Dallas, Texas 75275-0314, United States

Supporting Information

ABSTRACT: A total of 202 halogen-bonded complexes have been studied using a dual-level approach: ωB97XD/aug-cc-pVTZ was used to determine geometries, natural bond order charges, charge transfer, dipole moments, electron and energy density distributions, vibrational frequencies, local stretching force constants, and relative bond strength orders *n*. The accuracy of these calculations was checked for a subset of complexes at the CCSD(T)/aug-cc-pVTZ level of theory. Apart from this, all binding energies were verified at the CCSD(T) level. A total of 10 different electronic effects have been identified that contribute to halogen bonding and explain the variation in its intrinsic strength. Strong halogen bonds are found for systems with three-center-four-electron (3c-4e) bonding such as chlorine donors in interaction with substituted phosphines. If halogen bonding is supported by hydrogen bonding, genuine 3c-4e bonding can be realized. Perfluorinated diiodobenzenes form relatively strong halogen bonds with alkylamines as they gain stability due to increased electrostatic interactions.

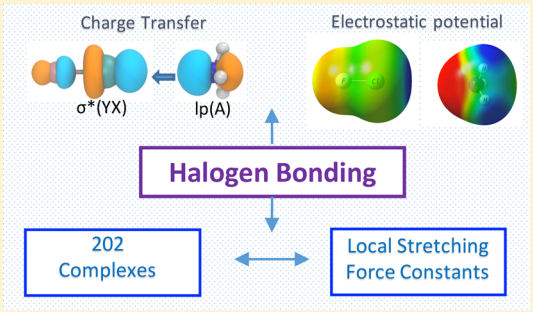

INTRODUCTION

Halogen bonding has been the topic of many excellent reviews,[1−11] summarizing a large number of experimental and computational investigations. The importance of this kind of noncovalent interaction for materials chemistry,[1,5,12−16] structural chemistry,[9,17−19] synthesis,[6,15,20] catalysis,[6,19,21,22] or medicinal chemistry[7,23] is well-documented. Halogen bonding involves the interaction between a halogen (X) and a Lewis base (A). We will abbreviate halogen bonding in the following by XB, where this abbreviation is also used for the adjective "halogen-bonded". It is generally accepted that quantum chemistry has been essential in understanding the various features of XB.[4,10,24−35] Most of the quantum-chemical investigations of the last years were based on density functional theory (DFT).[36−44] Other investigations used second-order Møller−Plesset perturbation theory[18,24,45,46,48−54] or more accurate methods.[28,32−35,38,55,56] In view of the many experimental and calculated data describing XB, it is safe to say that XB has many similarities with hydrogen bonding (HB):[57−62] Both involve a polarized H or X donor and a Lewis base with an occupied, relatively high-lying lone-pair (lp) orbital as the H or X acceptor A. Depending on the nature of the donor and acceptor, both HB and XB can vary from weakly electrostatic to strongly covalent interactions involving binding energies of 40 kcal/mol and more.[1−10] The strength of these interactions will depend on the complex geometry where a linear arrangement of HB or XB turns out to be energetically favorable. However, there is an important difference between HB and XB: The electronic nature of X should have a strong influence on the XB strength, and because X can vary from F via Cl, Br, I, to At, more possibilities for designing XBs with specific properties should exist.

Standard procedures use, e.g., the binding energies of XB complexes or structural parameters such as the distance between X and A as a measure of the strength of the XB.[2,63,64] More sophisticated approaches have utilized symmetry-adapted perturbation theory[20,47,52,65−70] or other energy decomposition methods[48,50,70] to obtain insight into the nature of XB. One has determined the electrostatic, exchange, and dispersion interactions adding to XB within a given model. Alternatively, one has analyzed wave-function and molecular orbitals, electron density, magnetic properties, electrostatic potential, or other properties to describe XB.[24,40,45−47,49,51,68,71−82] However, none of these properties provides a reliable measure of the intrinsic XB strength, which is decoupled from other interactions between the monomers. For example, by determination of the binding energy ΔE, all interactions between the monomers are included, and it is difficult to single out the energy associated with XB.[83,84] In this situation, vibrational spectroscopy helps because it is always possible to determine the local X···A stretching force constant, which provides a direct measure of the intrinsic bond strength.[85−88]

In previous investigations, we have used vibrational spectroscopy to determine the strength of the HB.[83,89−94] This was

Received: September 30, 2016
Published: December 14, 2016

DOI: 10.1021/acs.inorgchem.6b02358
Inorg. Chem. 2017, 56, 488−502

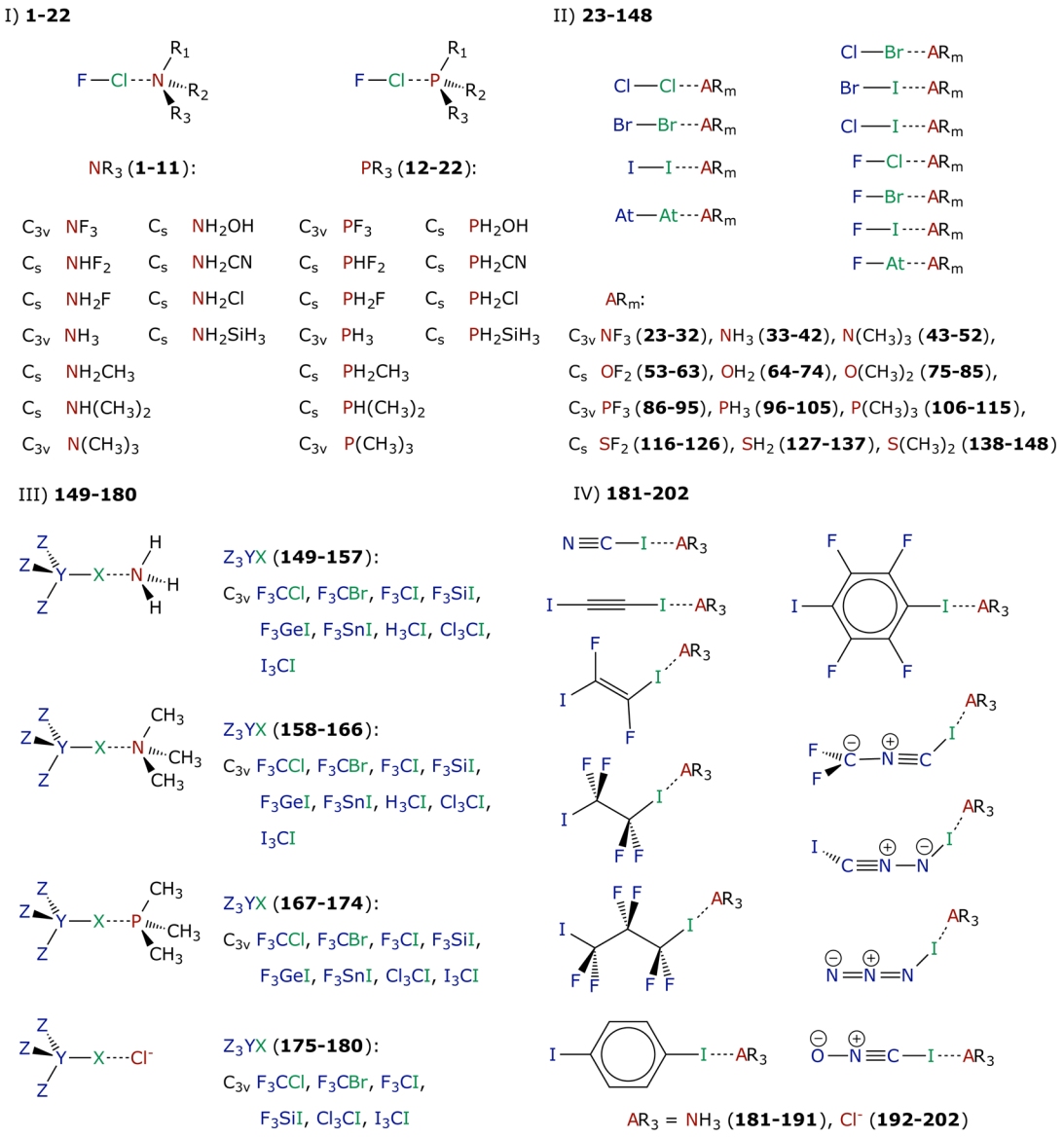

Figure 1. Schematic representations of complexes **1**−**202**.

done by using either experimental or calculated vibrational frequencies and solving for them the Zou−Cremer local equivalent of the Wilson equation to obtain local stretching force constants and frequencies.[87,88,95] Zou and Cremer have demonstrated that the local stretching force constant is directly related to the intrinsic bond strength[96] and therefore can be used as a sensitive measure to distinguish between the different types of HBs[83] or pnicogen bonds.[97,98] In this work, we will use vibrational spectroscopy to characterize the nature of the XB for a large variety of XB complexes by answering the following questions:

(i) Which XBs are weak and which are strong? Is there a relationship between the complex binding energy ΔE and the local XB stretching force constant k^a? (ii) To which degree does the XB strength vary in dependence of the Lewis base when the latter contains a heteroatom from the second (O and N) or third (S and P) period? (iii) How do Lewis base substituents affect the strength of the XB? (iv) How does the polarizability of a dihalogen X_2 or the polarity (dipole moment) of an interhalogen XY change the intrinsic strength of XB? (v) Can one determine the covalent and/or electrostatic character of XB with the help of calculated charge transfer (CT) or other properties of the XB complex? (vi) 3c-4e bonding, as is found for trihalogenide ions such as $[F_3]^-$, should also play a role for XB complexes. Can one quantify the degree of 3c-4e bonding and explain under which circumstances it can be expected for XB? (vii) How do relativistic effects change XB? (viii) Which haloorganic molecules form the strongest XB complexes? (ix) Can one work out design strategies for new useful materials based on XB? (x) Is it possible to order and compare on a quantitative basis XB if different atoms X and A throughout the periodic table interact?

These questions will be answered by investigating 202 neutral and anionic XB complexes, which are divided into groups, as shown in Figure 1. In section 2, we shortly describe the quantum-chemical methods and tools used in this work to investigate XB. Electronic effects, being decisive for XB, will be discussed in section 3, where the focus is on the role of the halogen and halogen acceptor. In section 4, we will analyze XB for halotetragens interacting with amines and phosphines. Finally, in section 5, we will draw the conclusion of this

DOI: 10.1021/acs.inorgchem.6b02358
Inorg. Chem. 2017, 56, 488−502

investigation and provide an outlook on how the results of this work can be used in the future.

COMPUTATIONAL METHODS

A two-pronged strategy was pursued to obtain a reliable description of the local vibrational modes of the 202 XB complexes investigated in this work. For this purpose, a subset of 28 complexes was investigated employing CCSD(T) (coupled-cluster theory with all singles, doubles, and perturbative triple excitations)[99] and Dunning's augmented triple-ζ basis sets aug-cc-pVTZ,[100−102] which contain diffuse basis functions to describe the charge distribution of anions and heteroatoms and the dispersion interactions in noncovalently bonded complexes. For atoms Br, I, At, and Sn, scalar relativistic effects were assessed by using effective core potentials (ECPs) in combination with the Dunning basis sets.[103] The CCSD(T) calculations were carried out employing a convergence criterion of 10^{-9} for the CC amplitudes. Various DFT methods were tested for their ability to reproduce the CCSD(T)/aug-cc-pVTZ results. All DFT calculations were performed with tight convergence criteria [self-consistent field, 10^{-10}; geometry iterations and forces, 10^{-7} hartree/bohr] and an ultrafine grid.[104] It turned out that ωB97X-D[105,106] leads to a better agreement with regard to the CCSD(T) results than, e.g., B3LYP,[107,108] PBE0,[109,110] or M06-2X.[111] However, even in the case of the ωB97X-D/aug-cc-pVTZ calculations, significant differences with the CCSD(T)/aug-cc-pVTZ results were found. The data reflecting these differences are given in Table S2 and Figure S1. They reveal the following.

The largest discrepancies are found for XB complexes between F_2 or FCl and a Lewis base containing third-period atoms such as S or P. For F_2 complexes, the stability is underestimated by ωB97X-D, whereas it is overestimated for the more stable FCl-amine and -phosphine complexes by maximally 2.9 kcal/mol. Percentage-wise deviations in the complex binding energies are generally not large and can be tolerated apart from the complexes mentioned. This holds also for the interaction distances r(XA) with the exception of $F_2\cdots OH_2$ and FCl···PF_3. However, the more sensitive second-order response properties such as the local stretching force constants reveal the deficiencies of the ωB97X-D/aug-cc-pVTZ description in half of the 28 complexes investigated. Especially problematic is the lack of accuracy of the k^a values in the cases of F_2 and F_3^-, which were the first choice of reference molecules with defined bond orders (1.00 and 0.50; see below).

Clearly, ωB97X-D is unable to describe F_2 and $[F\cdots F\cdots F]^-$ with the accuracy needed for this investigation. Therefore, we excluded these molecules and complexes containing F_2 from the DFT investigation. This implied that in this work FCl and $[F\cdots Cl\cdots F]^-$ were used as reference molecules (assumed bond orders 1.00 and 0.50; see below) to set up bond strength order (BSO) values. These are derived from the local stretching force constants, which were obtained utilizing the Konkoli−Cremer method that converts normal-mode frequencies ω_μ and force constants k_μ of a quantum-chemical calculation into local-mode frequencies ω_n^a and force constants k_n^a (μ, n = 1, ..., $3N - L$ with N = number of atoms and L = number of translations and rotations) using the local equivalent[85−88] of the Wilson equation of vibrational spectroscopy.[112]

According to the calculated Mayer bond orders[113,114] for FCl and $[F\cdots Cl\cdots F]^-$ (0.994 and 0.581, respectively), it is reasonable to assume that these are 1.00 and 0.50, where the latter is the result of 3c-4e delocalization and the occupation of all-bonding and nonbonding orbitals. By using these bond orders as reference BSO values and assuming that, for a stretching force constant k^a of zero, a zero BSO value results, the constants a and b in the power relationship[91,115]

$$n = a(k^a)^b \tag{1}$$

were determined to be 0.380 and 0.611, respectively. The corresponding CCSD(T) values are a = 0.387 and b = 0.649, which confirms the usefulness of the ωB97X-D/aug-cc-pVTZ calculations provided F_2 complexes are eliminated from the investigation. By determination of the BSO value n(X···A) = n(XB) for each calculated k^a(X···A), an easy ordering and comparison of XBs according to their intrinsic strength becomes possible.

Because 3c-4e bonding can occur, its magnitude was assessed in percentage with the help of the ratio n(X···A)/n(XY) × 100. If this ratio leads to unity, 3c-4e bonding is fulfilled by 100% as in $[F\cdots Cl\cdots F]^-$. Values below 40% indicate that 3c-4e bonding plays a minor role. Values above 100% suggest an inverse 3c-4e bond where the XA interactions (i.e., the XB) are stronger than the XY interactions. Values above 100% are listed in the tables to quickly identify inverted 3c-4e bonding but are compared with other values via their reciprocal. In addition to the BSO test, the XY and XA distances were compared with the corresponding values in the appropriate monomers.

Binding energies ΔE were calculated at the ωB97X-D/aug-cc-pVTZ level, where the counterpoise correction of Boys and Bernardi[116] was used to correct for basis set superposition errors (BSSEs). For each of the 202 complexes investigated, the BSSE-corrected CCSD(T)/aug-cc-pVTZ binding energy was also calculated to provide an estimate of the reliability of the ωB97X-D/aug-cc-pVTZ calculations (see Table S1 and Figure S2). For this purpose, DLPNO−CCSD(T)[117,118] and the def2-TZVP basis sets[119] in conjunction with the Stuttgart−Dresden ECPs for iodine[120] were used.

The local properties of the electron density distribution, $\rho(\mathbf{r})$, and the energy density distribution, $H(\mathbf{r}) = G(\mathbf{r}) + V(\mathbf{r})$ [$G(\mathbf{r})$ = kinetic energy density (positive, destabilizing); $V(\mathbf{r})$ = potential energy density (negative, stabilizing)], were computed at the ωB97X-D/aug-cc-pVTZ level of theory. The Cremer−Kraka criteria for covalent bonding were applied.[121−123] These associate a negative and therefore stabilizing energy density at the bond critical point $\mathbf{r}_b$ [$H(\mathbf{r}_b) = H_b < 0$] with dominating covalent character, whereas a positive (destabilizing) energy density ($H_b > 0$) is associated with predominant electrostatic interactions.

The covalent character of XB was also assessed by calculating the delocalization energy ΔE(del) = ΔE[lp(A)→$\sigma^\star$(XY)], which is associated with CT from the lp(A) (Lewis base) to the antibonding $\sigma^\star$(XY) orbital (halogen donor), thus leading to an increase of the electron density in the XB region. The magnitude of ΔE(del) was determined by second-order perturbation theory.[124] Detailed analysis of calculated atomic and monomer charges reveals that CT from the halogen acceptor to the halogen donor is largely dominated by the lp(A) → $\sigma^\star$(XY) transfer but is not the only CT. Also, there are other covalent contributions to XB according to the natural bond order (NBO) perturbation analysis. However, ΔE(del) turned out to be the most important contribution in line with frontier orbital theory, and therefore we considered the intermonomer CT calculated in this work as the "lp(A) → $\sigma^\star$(XY)" CT for reasons of simplicity.

Electrostatic interactions were determined by investigating the electrostatic potential $V(\mathbf{r})$ on the 0.001 e/bohr^3 electron density surface of the monomers listed in Tables S3 and S4. For halogen donors, the $V(\mathbf{r})$ maximum in the nonbonding region in the σ direction (σ-hole-attracting negative charge) and, for halogen acceptors (Lewis bases), the $V(\mathbf{r})$ minimum in the lp region were calculated. These values are given in the SI in kilocalories per mole and provide a measure for electrostatic attraction.[125−128]

Calculation of the local-mode properties was carried out with the program *COLOGNE2016*.[129] CCSD(T) energies were obtained with the packages *CFOUR*[130] and *ORCA*.[131] For NBO analysis, *NBO 6*[124] was used, whereas the electron (energy) density distribution was analyzed with the program *AIMAll*.[132] DFT calculations were performed with the package *Gaussian09*.[133]

RESULTS AND DISCUSSION

A schematic representation of the 202 molecules investigated in this work is given in Figure 1. They are separated into four groups (I−IV). Investigation of the FCl complexes of group I (**1**−**22**), which involve amines and phosphines, provides a possibility of studying the consequences of halogen acceptor substitution for the strength of XB. Group II (**23**−**148**) contains dihalogens X_2 and interhalogens XY interacting with acceptors AR_m (R = F, H, CH_3; m = 2, 3), with A being an

DOI: 10.1021/acs.inorgchem.6b02358
Inorg. Chem. 2017, 56, 488−502

atom of the second or third period (O and N or S and P). Group II is included to study the influence of the polarizability of X and the polarizing power of Y on XB. Groups III (**149**−**180**) and IV (**181**−**202**) contain the actual targets of this work: Simple halomethanes and halotetraganes interacting with amines, phosphines, or the Cl^- anion are contained in group III. Group IV consists of organoiodine molecules interacting with Cl^- or NH_3.

In view of the large number of molecules investigated, the data for all monomers and XB complexes (see Figure 1) are summarized in Table S2, which contains bond lengths r(YX) and r(X···A) in Å, binding energies ΔE(DFT) and ΔE[CCSD(T)] in kcal/mol, electron density ρ_b at the XB critical point in electron/bohr^3, energy density H_b at the XB critical point in hartree/bohr^3, delocalization energies ΔE(del) = ΔE(lp→$\sigma^\star$(XY)) in kcal/mol, intermonomer CT dominated by the transition lp(A)→$\sigma^\star$(XY) in electrons, local stretching force constants k^a(XY) and k^a(XB) = k^a(X···A) in mdyn/Å, BSO values n(XY) and n(XB) = n(X···A), the degree of 3c-4e bonding in %, and the frequency of that normal mode, which has dominant XB stretching character. The latter is given to provide vibrational spectroscopy information, where the XB stretching band should be found when either IR or Raman spectra are recorded. Tables S3 and S4 contain molecular properties of the XB acceptors and donors, respectively. Figures S3−S5 provide a schematic representation of all complexes with NBO charges.

Rather than a discussion in detail of the data collected in the Supporting Information (SI), the most important results are given in the form of suitable diagrams. Figure 2 summarizes all

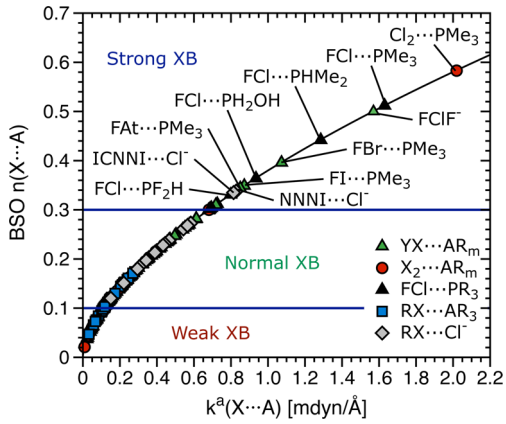

Figure 2. Power relationship between the relative BSO n and the local stretching force constants k^a of XB complexes **1**−**202** given according to eq 1 (solid black line). Weak, normal, and strong XB are separated by the horizontal blue lines.

results in a BSO diagram, which shows that XB can vary from very weak ($n \leq 0.1$) to rather strong interactions ($n \geq 0.3$), which are found for some phosphine complexes. The sequence of increasingly stronger XB shown in Figure 2 and given in more detail in Table S2 provides for the first time a quantitative comparison of the various types of XB.

In Figure 3, the nature of the XB is characterized with the help of the energy density H_b at the XB critical point. There is a variation from electrostatic (H_b values close to zero) to covalent bonding with distinctly negative H_b values that indicates stabilization of the electron density at the XB critical point and, by this, covalent interactions according to the Cremer−Kraka criteria.[121] Analysis of the energy density is confirmed by the corresponding CT values from the lp(A) orbital to the $\sigma^\star$(XY) orbital, and the corresponding delocalization energies are listed in Table S2.

Figure 4 provides analysis of FCl-amine and FCl-phosphine complexes, again based on the BSO values determined with eq 1. Figures 5 and 6 compare XB for various halogens and interhalogens (excluding the F_2 complexes for the reasons discussed above) in combination with second- and third-row heteroatoms A that characterize a given type of Lewis base. XBs for halomethanes, in general, and iodocarbons, specifically, are analyzed in Figures 7 and 8.

A possible relationship between the intrinsic bond strength of XB and the complex binding energy ΔE (Figure 9) or the delocalization energy ΔE(lp→$\sigma^\star$(XY)) (Figure 10) is also investigated. In the SI, similar relationships with the electron density ρ_b and acceptor ionization potentials (IPs) are provided.

These results lead to a clear picture of the nature of XB, which can be rationalized by considering 10 different electronic effects. Most of them have been previously discussed in connection with XBs (orbital energy and overlap,[36,37,44,53] electrostatic effects and σ-hole influence,[46,125−128,134−136] and CT[41,137]). However, in this work we summarize these electronic effects in a compact way, applying vibrational spectroscopy and the local vibrational modes.

1. *Changes in the orbital energy of lp(A) and the electronegativity of A.* Covalent contributions sensitively depend on the lp(A) energy that influences the orbital energy difference $\Delta\epsilon$ = ϵ[lp(A)] − ϵ[$\sigma^\star$(XY)] with ϵ[lp(A)] < ϵ[$\sigma^\star$(XY)]. The smaller $\Delta\epsilon$ is, the larger are the CT and covalent contributions. Trends in ϵ[lp(A)] are reflected by the corresponding vertical IPs (see the SI) or, more directly, by the calculated lp(A) orbital energies. For a third-row element like P, the lp orbital is lying higher in energy and by this the covalent contribution is larger, as confirmed by the BSO values of the phosphine and amine XB complexes shown in Figure 4.

1a. *Orbital energy of lp(A) and σ-withdrawing/donating groups at A.* The lp(A) orbital can be raised by suitable substituents to decrease $\Delta\epsilon$. As shown in Figure 4 (amines in red; phosphines in green), the XB strength ranges from BSO values n = 0.100 for FCl···NF_3 to 0.270 for FCl···$N(CH_3)_3$, whereas for the phosphines, the bond strength varies from n = 0.064 (FCl···PF_3) to n = 0.512 (FCl···$P(CH_3)_3$), thus revealing that the strength of the XBs formed with FCl largely depends on the halogen acceptor. For amines, the XB strength increases in the series NF_3 < NHF_2 < NH_2CN < NH_2F < NH_2Cl ≈ NH_2SiH_3 < NH_3 < NH_2OH < NH_2CH_3 < $NH(CH_3)_2$ < $N(CH_3)_3$. For phosphines, the intrinsic strength of XB increases as follows: PF_3 ≈ PH_2CN < PH_3 < PH_2SiH_3 < PH_2Cl < PH_2F ≈ PH_2CH_3 < PHF_2 < PH_2OH ≪ $PH(CH_3)_2$ < $P(CH_3)_3$. Electron-withdrawing substituents such as F in NF_3 lower ϵ[lp(A)] and thereby weaken XB, whereas electron-donating groups such as Me raise ϵ[lp(A)] and thereby strengthen the covalent contribution to XB.

1b. *Orbital energy of lp(A) and π-withdrawing/donating groups at A.* Substituents, which lead to a potential delocalization of lp(A) such as the cyano group in PH_2CN, lower ϵ[lp(A)], increase $\Delta\epsilon$, and thereby weaken XB (see **20** in Table S2). π-Donating substituents such as Cl in chlorinated phosphines have destabilizing pπ,lp(A) 4e interactions that cause an increase of ϵ[lp(A)]. The latter effect can be stronger than the σ-electron-withdrawing effect so that the Lewis base becomes a

DOI: 10.1021/acs.inorgchem.6b02358
Inorg. Chem. 2017, 56, 488−502

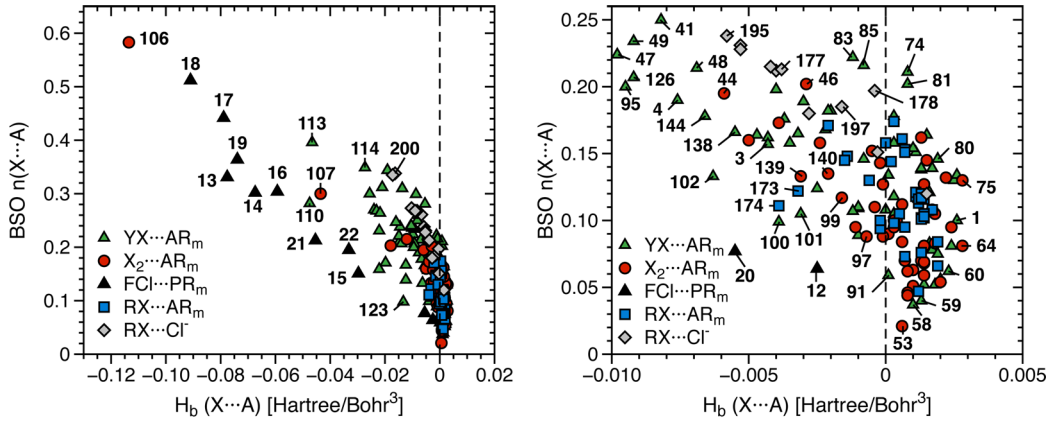

Figure 3. (a) Comparison of the BSO n with the energy density H_b at the density critical point of the XB for complexes **1**−**202**. (b) Enlargement of the range $0 < n < 0.026$; $-0.010 < H_b < 0.005$ hartree/bohr^3. Electrostatic XBs are indicated by $H_b \geq 0$, whereas negative H_b values are associated with covalent XB.[121,122] For the numbering of XB complexes, see Tables S2, S7, and S8.

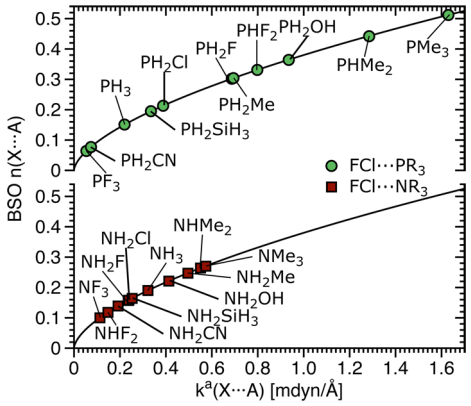

Figure 4. Relationship between the relative BSO n and the local XB stretching force constant k^a (eq 1; solid black lines) for XB complexes involving FCl as halogen donor and amines (lower curve, red squares) or phosphines (upper curve, green dots) as halogen acceptors.

stronger electron donor. For phosphines, these effects dominate, whereas for amines, the Cl substituent acts more as a σ acceptor rather than a π donor. The calculated strength of XB in the FCl complexes of NH_3 (n = 0.190), NH_2CN (0.139), NH_2Cl (0.158) and PH_3 (0.151), PH_2CN (0.077), $P(CN)_3$ (0.044), PH_2Cl (0.213), and PCl_3 (0.096) confirms these effects (see Table S2 and Figure 4). Noteworthy is that the sensitivity of XB to substituent effects in the Lewis base is much larger for third rather than second period atoms A, which is especially obvious for the phosphines.

2. *Orbital overlap between X and A.* Covalent bonding requires an efficient overlap between the interacting orbitals, i.e., the lp(A) and $\sigma^\star$(XY) orbitals. The latter depends on the geometry of the complex [a linear arrangement of the unit (A, centroid of lp, X, and Y) would be optimal as well as a short interaction distance r(X···A)], the nodal characteristics of the valence orbitals, and their diffuseness. The rule of thumb is that orbital overlap decreases when the principal quantum numbers of X and A increasingly differ and/or the electronegativity difference $\Delta\chi(A,X) = \chi(A) - \chi(X)$ increases. Electronegative substituents at an atom A with a diffuse lp (e.g., P) can improve the overlap due to orbital contraction. The best overlap can be expected between atoms belonging to the same period and having similar χ values. The overlap decreases in the series ClCl, ClBr, and ClI or in the series FF, FCl, FBr, FI, and FAt, as is in line with the

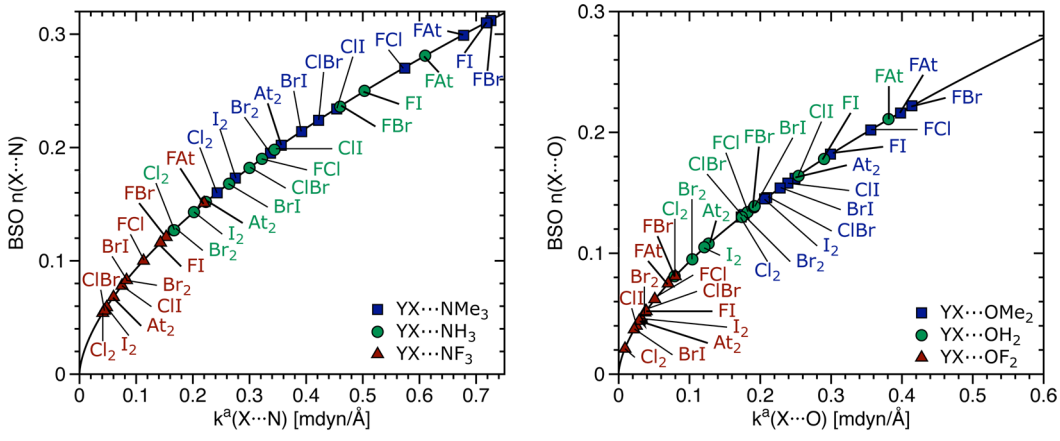

Figure 5. Relationship between the relative BSO n and the local XB stretching force constant k^a (eq 1; solid black lines) for dihalogens and interhalogens interacting with (a) amines NF_3, NH_3, and NMe_3 and (b) OF_2, OH_2, or OMe_2.

DOI: 10.1021/acs.inorgchem.6b02358
Inorg. Chem. 2017, 56, 488−502

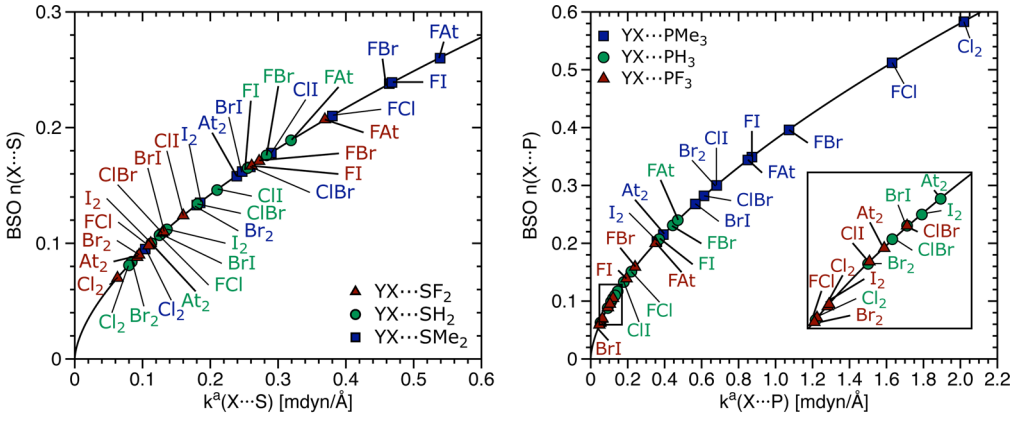

Figure 6. Relationship between the relative BSO n and the local XB stretching force constant k^a (eq 1; solid black lines) for dihalogens and interhalogens interacting with (a) SF_2, SH_2, and SMe_2 and (b) PF_3, PH_3, or PMe_3.

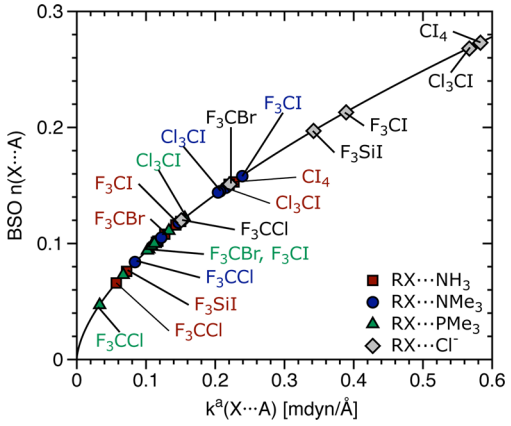

Figure 7. Relationship between the relative BSO n and the local XB stretching force constant k^a (eq 1; solid black line) for complexes involving halotetragenes and four different acceptors (NH_3, red squares; NMe_3, blue circles; PMe_3, green triangles; Cl^-, gray diamonds).

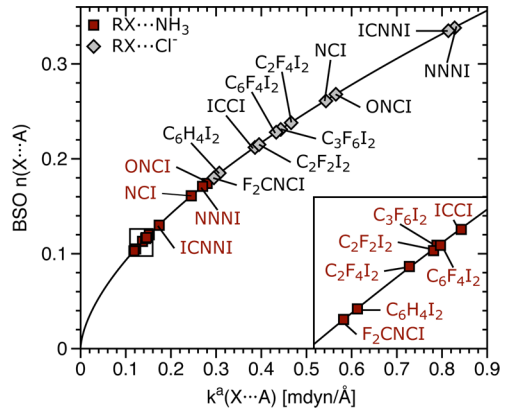

Figure 8. Relationship between the relative BSO n and the local XB stretching force constant k^a (eq 1; solid black lines) for XB complexes involving various organoiodine molecules and Cl^- and NH_3 as acceptors.

calculated BSO values. In this connection, one always has to consider the orbital orthogonality between the σ(XY) and $\sigma^\star$(XY) orbitals. It is important to understand [lp-(A)−$\sigma^\star$(XY)] overlap and the formation of 3c-4e-bonding (see below).

3. *Relativistic effects on the orbital overlap and energy.* Scalar relativistic effects lead to a contraction of valence s and p orbitals of relativistic atoms such as X = Br, I, or At.[138] Orbital contraction implies that the energy of the bonding and antibonding XY orbitals is somewhat lowered, and the effective electronegativity χ of X is raised, where both effects slow down the increase of $\epsilon(\sigma)$ with decreasing χ and the nonrelativistic decrease of χ with the atomic number AN within a group. Orbital contraction (strong for s and weak for p if spin−orbit effects are averaged) implies also a reduced (anti)bonding XY and reduced [lp(A)−$\sigma^\star$(XY)] overlap. In the series FCl, FBr, FI, and FAt, the BSO value decreases from the reference n(FCl) = 1.00 to n(FAt) = 0.827 (Table S4). CT from the lp(A) of a Lewis base to the $\sigma^\star$(XY) orbital and the covalent character of XB decreases less drastically for Br, I, and At because of the scalar relativistic effects.

4. *Strengthening of XB by 3c-4e-bonding.* Anions F_3^-, Cl_3^-, $FClF^-$, etc., undergo XB in the sense of a 3c-4e bond, where, according to molecular orbital theory, a covalent XB bond order of 0.5 results. In these complexes, the outer atoms are negatively charged, whereas the inner atom is less negatively or slightly positively charged. If a Lewis base is carrying an electron-withdrawing substituent (preferably F but also OH, Cl, CN, etc.), XB can lead to partial 3c-4e character, which is given in this work in percentage (see Table S2). This is low if amines, ethers, or thioethers are involved but increases for phosphines with electron-donor substituents to 100% and beyond, indicating inverted 3c-4e bonding. For FCl···PH_2OH (**19**), a perfect 3c-4e bond is observed, which is the result of a peculiar interaction between XB and HB (see below). This electronic effect was first discussed by Alkorta and co-workers[45] and called *chlorine shared bonds*. We hesitate to use this term because it suggests a new type of bonding, which is nothing else but the well-known 3c-4e bond (or Rundel−Pimentel bonding[28,139,140]).

5. *Halogen transfer and ion interactions.* Strong covalent character associated with a large CT from A to X leads to a breaking of the XY bond and the transfer of X^+ to AR_m. This happens for phosphine complexes FCl···$PHMe_2$ (**17**), FCl···PMe_3 (**18**), ClCl···PMe_3 (**106**), and BrBr···PMe_3 (**107**), which might be considered as phosphonium halogenide complexes that are stabilized by ion−ion attraction (see charges in the SI).

DOI: 10.1021/acs.inorgchem.6b02358
Inorg. Chem. 2017, 56, 488−502

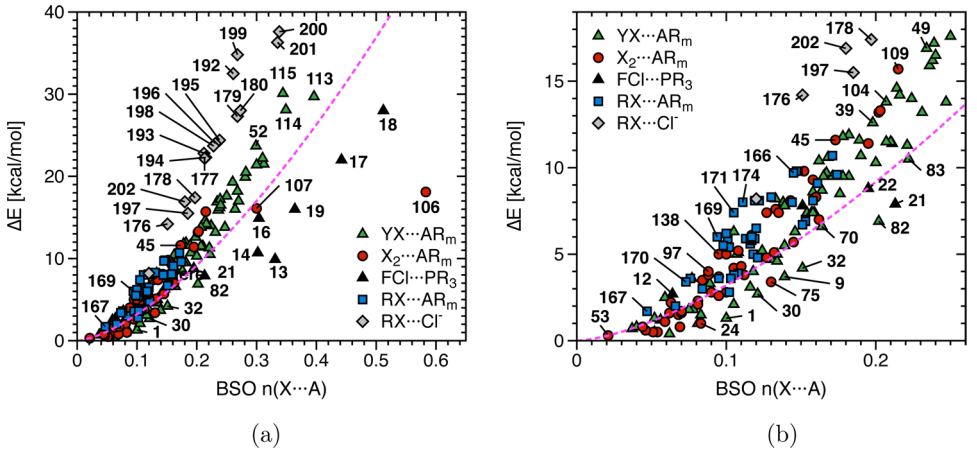

Figure 9. Comparison of the BSO n values and the binding energy ΔE for (a) complexes **1**−**202**. (b) Enlargement of the region $0 < n < 0.026$; $0 < \Delta E < 19$ kcal/mol. The purple line indicates the expected relationship between the two quantities. For the list of complex numbers, see Tables S2, S9, and S10.

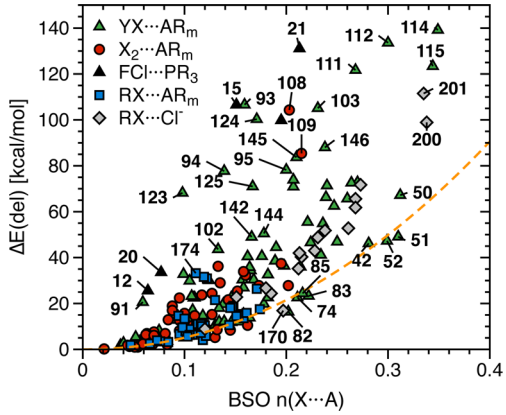

Figure 10. Comparison of the second-order CT stabilization energy $\Delta E(\text{del}) = \Delta E[\text{lp(A)}\rightarrow\sigma^{\star}\text{(XY)}]$ and the BSO n values. The yellow line provides a reference line (see the text). Complexes with 3c-4e bonding have large $\Delta E(\text{del})$. Complexes with strong 3c-4e bonding or phosphonium character are not included.

Because the phosphonium ion complexes also have 3c-4e bonding character (the percentages given in Table S2 are >100 and have to be inverted: 100/115 = 87, 68, 43, and 81%), their PCl bond is labilized, and only ClCl···PMe_3 can be considered to be dominated by phosphonium character. In this work, the classification as an ion pair was first based on the YX and XA distance analysis using the corresponding monomer distances of di/interhalogens and phosphonium ions as reference (Table S5). Subsequently, it was revised by utilizing the corresponding BSO values (Table S6), which are more reliable. Accordingly, Cl^{-}···$ClPMe_3^{+}$ is the only system with sufficient ion-pair character, where bonding takes place in the form of noncovalent dihalogen interactions between the Cl anion and a positively charged Cl in the phosphonium ion. This situation is generally considered as XB and can be contrasted with fully delocalized 3c-4e systems such as $[F\cdots Cl\cdots F]^{-}$ or FCl···PH_2OH (**19**), which are also considered to be stabilized by XB.

6. *Charge attraction/repulsion between X and A.* Coulomb attraction between a negatively charged A and a positively charged X stabilizes XB. For an interhalogen XY, with Y being the more electronegative atom, CT from X to Y leads to bond polarity and a positively charged X atom. If the electronegativity difference $\Delta\chi(\text{Y,X}) = \chi(\text{Y}) - \chi(\text{X})$ increases (e.g., in the series FCl to FAt), the charge of X increases and thereby X−A attraction exists. Similarly, the negative charge of A can be increased by electron-donating substituents so that Coulomb attraction increasingly supports XB. Noteworthy is that XB in FCl-phosphine complexes is relatively strong despite a charge repulsion between a positively charged X (because of the higher electronegativity of F) and a positively charged P (see Figure S3 and the following).

7. *Role of a σ hole at X and the electrostatic potential.* Charge repulsion between X and A, as suggested by the calculated NBO charges, does not consider the anisotropy of the electron density distribution. The negative charge of X screens the nucleus less in the XY bond (σ direction), thus leading to positive values of the electrostatic potential V when V is calculated outside the bond region for the 0.001 e/bohr^3 electron density surface (henceforth called the van der Waals surface). This is generally interpreted as a σ hole. The importance of σ-hole,lp interactions is well-established.[125−128] The σ hole of X in interhalogens XY increases with the polarity of the XY bond, which increases with increasing $\Delta\chi$(Y,X) [Allred−Rochow χ values are 4.10 (F), 2.83 (Cl), 2.74 (Br), 2.21 (I), and 1.90 (At)[141,142]]. Similar trends can be found for the interhalogens (Table S4). Accordingly, XB is influenced by the σ hole of X in XY, as is reflected by an increase of the XB BSO values in the series $X_2\cdots AR_m$ and $FX\cdots AR_m$ (X = Cl, Br, I, At; AR_m = OH_2, NH_3; see Table S2).

8. *Dipole−dipole interactions between XY and AR_m.* Electrostatic attraction between X and A can be influenced if the molecular dipole moments are collinearly aligned as in FCl···NH_3, whereas dipole−dipole repulsion in a complex influences the XB in FCl···PH_3. Because of this, the dipole moments of the monomers are listed in the Tables S3 and S4. Noteworthy are the large dipole moments of NH_2CN (4.61 D, Table S2) and PH_2CN (3.70 D), which are arranged in a direction that leads to repulsion with the FCl dipole (0.86 D).

9. *Mutual polarization XY and AR_m.* Interaction between the multipole moments of the monomers (here only atomic charges and dipole moments are considered) is enhanced by induced electrostatic interactions. These depend on the polarizability of the monomers and their polarizing power. The first property is a tensor where for reasons of simplicity here just the isotropic polarizability α_{iso} is considered (see Table S4), although a more detailed analysis might focus on the

DOI: 10.1021/acs.inorgchem.6b02358
Inorg. Chem. 2017, 56, 488−502

σ polarizability. The value of α_{iso} increases steeply in the series F_2 (8.2 bohr^3), Cl_2 (30.6), Br_2 (45.4), I_2 (71.6), and At_2 (87.4), thus explaining why Cl_2 and higher halogens are so easily polarized, which will lead also to an increase of the X σ hole by a Lewis base with sufficient polarizing power. This can be estimated by calculating V at a position on the van der Waals surface of A, which is next to X and gives a measure for the effect of the lp(A) electrons. The more negative V is for lp(A) (see Table S3), the stronger should be the polarizing power of the Lewis base. The negative value of V increases with (i) χ(A) (amines have more negative values than phosphines) and (ii) the electron-donating power of R in AR_m. More positive values of V at the position of lp(A) are obtained if the lp electrons are delocalized as for CN substituents or when R has a much larger electronegativity than A (as in PF_3).

10. *Augmentation of XB by HB.* There are some interesting exceptions to effects 1 and 2: An OH group does not lead to a weakening of the XB but to its strengthening ($FCl\cdots PH_2OH$: n = 0.364 compared to n = 0.304 for $FCl\cdots PH_2CH_3$). Inspection of the geometry of $FCl\cdots PH_2OH$ reveals that this unusual behavior of the OH group is due to HB with Cl, which increases the complex stability. If the HB is broken by rotation of the OH group, the hydroxyl group functions, as expected, as an electron-withdrawing group with a XB weakening effect.

Clearly, electronic effects 1−5 are relevant for the covalent part of XB, whereas effects 6−9 concern the electrostatic part. Additional electronic effects can augment either covalent or electrostatic XB. It is well-known that exchange repulsion and dispersion forces influence the strength of XB.[68,143] Furthermore, spin−orbit coupling plays a significant role for atoms such as Br, I, and At.[144−146] These additional effects were not explicitly calculated in this work but have to be considered in the following.

Before some classes of XB complexes are discussed in more detail, it is appropriate to differentiate between physically based observables and the model quantities used in this work. Clearly, the local mode frequency can be measured[88] and the local force constants can be derived from the former. This is also true for the electron density or the dipole moment, whereas NBO charges are orbital-based and therefore model quantities. A chemist wants to explain XB in terms of covalent, exchange, electrostatic, inductive, and dispersion interactions. Politzer and co-workers[147−149] have recently pointed out that according to the Hellmann−Feynman theorem[150] noncovalent interactions are purely Coulombic in nature and include polarization and dispersion. Therefore, noncovalent interactions such as XB may be described purely on the basis of Coulomb interactions. Although this is a valid view, it does not exclude that one uses model quantities such as NBO charges, CT values, or charge delocalization energies for a more detailed, model-based description of XB. We will use the CT values as an indicator of covalent bonding, where one has to realize that within the model used smaller contributions to CT might also arise from other than covalent interactions. In a similar way, we will use an energy-density-based model that distinguishes just between covalent and electrostatic forces.[121−123]

XB with Phosphines. Considering all effects, the strong covalency of XB in phosphine complexes (Table S2 and Figure 3) is noteworthy. This can lead to BSO values larger than 0.3 (1), where, as shown above, especially methyl substituents help to increase the intrinsic XB strength. For $P(CH_3)_3$, the lp(P) orbital energy is raised [CCSD(T): IP = 8.6 eV; IP(PH_3) = 10.5 eV; Table S3] via hyperconjugation and a lower electron-withdrawing effect of the methyl group. The very low value of V [$V(PMe_3)$ = −28.8 kcal/mol; $V(PH_3)$ = −16.9 kcal/mol] and the high polarizability (PMe_3, 67.6 bohr^3; $\alpha_{iso}(PH_3)$, 30.8 bohr^3; Table S3) cause both the covalent and electrostatic parts of XB in, e.g., $FCl\cdots PMe_3$ (ΔE = 28.0 kcal/mol; n(XA) = 0.512; Table S2), to be relatively large and the complex to take the character of a chlorophosphonium ion interacting with F^- via significant 3c-4e bonding (68%).

In the series Cl_2, Br_2, I_2, and At_2 or FCl, FBrl, FI, and FAt, the electrostatic interactions with $P(CH_3)_3$ increase in a limited way because of an increasing σ hole and an increasing polarizability of X but an increased repulsion between positively charged X and P (Tables S3 and S4 and Figure S4). At the same time, the covalent contributions decrease because of an increase in the $\sigma^\star$(XY) energy and a decrease of the orbital overlap, as is documented by the CT values in Table S2. Accordingly, for Cl_2 and FCl, the strongest XB is found (n = 0.583 for **106** and n = 0.512 for **18**), indicating in the first case a phosphonium complex with 3c-4e character and in the second case inverted 3c-4e character.

Using the 10 electronic effects discussed above, the trends in the intrinsic strength of XB, as reflected by the BSO values shown in Figures 3−6, can be explained in detail. The insight provided by these values makes it possible to discuss XB for halogenated carbon molecules, which are directly relevant for polymer chemistry and materials science.

■ ASSESSMENT OF XB INVOLVING TETRAGENES

The lower electronegativity of carbon compared to that of the halogens leads to higher orbital energies σ(XY) and $\sigma^\star$(XY) and to reduced overlap between the latter and the lp(A) orbital. The polarity of the CX bond is inverted (compared to FCl) and causes a larger (smaller) orbital coefficient of X in the σ(CX) bonding [$\sigma^\star$(CX) antibonding] orbital. Hence, 4e repulsion between lp(A) and σ(CX) will be larger and 2e stabilization between lp(A) and $\sigma^\star$(CX) lower. This can be directly verified by the reduced CT and ΔE(del) values of the halocarbons (Table S2). Halocarbons lead to weak electrostatic XB. To increase the intrinsic strength of the XB involving a halocarbon, the effective electronegativity of the C(X) carbon has to be increased, which is accomplished by halogenation. Apart from this, it is interesting to see how XB is changed when halomethanes are replaced by the corresponding silanes, germanes, and stannanes. For this purpose, a set of tetraganes interacting with NH_3, NMe_3, PMe_3, and the Cl^- anion as halogen acceptors were investigated. The calculated BSO values of the halomethanes are shown in Figure 7.

XB for Halomethanes and Halotetraganes. According to the calculated BSO values, both weak and normal XB are observed, where the largest BSO values are obtained for the Cl^- anion (0.120−0.273 corresponding to ΔE values from 8.2 to 28.0 kcal/mol; Table S2), which indicates how anions as halogen acceptors significantly increase the strength of XB. Different from what was found for dihalogens and interhalogens, halocarbons form XB with phosphines and, in particular, $P(CH_3)_3$, which have slightly lower strength (0.047−0.122) than those formed with NH_3 (0.066−0.153) and $N(CH_3)_3$ (0.084−0.158; Table S2). This reflects the smaller covalent character of the XB involving tetraganes as X donors. $P(CH_3)_3$ still leads to larger CT values (Table S2), but the corresponding XB strength is also influenced by electrostatic contributions such as X−A repulsion (attraction) determined by the

DOI: 10.1021/acs.inorgchem.6b02358
Inorg. Chem. 2017, 56, 488−502

calculated atomic charges, σ-hole−lp(A) attraction as reflected by the calculated V values, and charge polarizability.

According to the BSO values, σ-hole−lp(A) attraction seems to be decisive, as suggested by V values of −37.7, −30.9, and −28.8 kcal/mol for the lp(A) in NH_3, $N(CH_3)_3$, and $P(CH_3)_3$, respectively. Nevertheless, small covalent contributions remain to be important, as the BSO values of complexes with H_3CI, F_3CI, Cl_3CI, and CI_4 reveal, where Cl_3CI and CI_4 form stronger XB than F_3CI for both NH_3 and Cl^-. This can be related to a lowering of the lowest unoccupied molecular orbital (LUMO) of the halomethanes, as was already pointed out by Huber on the basis of binding energies.[53] The highest BSO values are obtained for Cl_3C−I as a halogen donor, which is because of its high polarizability (90.2 bohr^3; Table S4) and a positive charge at I, which is more attracted by the negatively charged N in NH_3 (−1.056 e) and $N(CH_3)_3$ (−0.500 e) than the positively charged P (1.123 e; Figure S3) in $P(CH_3)_3$. Similar considerations apply to F_3C−I and I_3C−I, which lead with $N(CH_3)_3$ to relatively strong XB complexes [ΔE = 8.3 and 10.3 kcal/mol (CCSD(T)].

When C is replaced with a less electronegative tetragene such as Si, Ge, or Sn [Allred−Rochow: χ(C) = 2.50 > χ(Ge) = 2.02 > χ(Si) = 1.74 ≃ χ(Sn) = 1.72[141,142]], the strength of the XB decreases, where the BSO follows the changes in the σ-hole potential value (see Tables S2 and S4) and the fact that X becomes increasingly negatively charged. Again, the strongest values are found for the iodomethanes. This clarifies that once the interaction between R_mCX and a Lewis base is considered, it is limited to the moderate donor ability of the halocarbon, where an iodocarbon provides the best option. Therefore, stronger XB can only be provided by increasing the polarity of the C−I bond via an increase of the effective electronegativity of C, an increase of the polarizability of the halogen donor, and/or modification of the Lewis base. As the examples involving the chloride anion reveal, enlarged BSOs of up to 0.3 (in this work considered as the border to strong XB) result, where both increases of the covalent [higher lp(A) energies and stronger CT] and electrostatic contributions (higher polarizability of the Lewis base; Table S3) play a role.

XB for Organoiodine Compounds. Because iodocarbons provide the strongest XB (among the tetragenes), an increase of the perfluorinated iodoalkane chain might be one possibility (**184**, **185**, **195**, and **196**) to strengthen the XB. However, the calculated BSO values reveal little improvement. The change in the effective electronegativity of C(I) is too small. A larger effect is obtained when *p*-diiodobenzene is perfluorinated. The BSO value increases from 0.105 (**186**) to 0.117 (**187**) and the binding energy from 3.8 to 6.0 kcal/mol where the increase of the σ hole from V = 22.0 to 32.9 kcal/mol seems to be the most important change. Perfluorinated *p*-diiodobenzene materials are already widely used in gels, fluorescent materials, and others.[16,151−153]

A larger change in the electrostatic potential V is accomplished in the series difluorodiiodoethene (**183**, V = 32.3 kcal/mol), diiodoacetylene (**182**; 37.6 kcal/mol), and iodocyanide (**181**; 51.8 kcal/mol; Table S4). If this is combined with increased covalent and electrostatic contributions, as provided by an anion such as Cl^-, then BSO values of 0.215, 0.212, and 0.261 can be obtained, where the switch in the order of the XB strengths is due to the covalent contributions and a relatively large CT of 0.188, 0.179, and 0.221 e (electron; ΔE(del) = 40.3, 35.2, and 52.8 kcal/mol; Table S2) in line with the LUMO energies. The corresponding binding energies are 22.4, 22.9, and 31.6 kcal/mol [CCSD(T); Table S2]. Obviously, iodocyanide is too toxic to work with, but diiodoalkynes could be used as suitable compounds to form polymers based on XB, as is already known for some time.[154−156]

XB of similar or even larger strength than the one found in iodocyanide is observed for ONCI, ICNI, and NNNI complexes. In the first case, the nitroso substituent leads to an increase in the polarizability of the X donor (from 48.7 bohr^3 for NCI to 59.8 bohr^3 for ONCI), resulting in a slightly stronger bond (BSO value of 0.174 compared to 0.161 for NCI···NH_3), whereas for ICNI and NNNI, the higher electronegativity of N compared to C [χ(C) = 2.50; χ(N) = 3.07] lowers the energy of σ(NI) and $\sigma^\star$(NI) and improves the lp(A)−$\sigma^\star$(NX) overlap, which results in larger CT and ΔE(del) values compared to the ones found for iodocarbon complexes (Table S2). Although ICNI and NNNI have a lower electrostatic potential than NCI (V = 38.4 and 42.4 kcal/mol compared to 51.8 kcal/mol), they are capable of forming XB of similar strength for NH_3 (BSO values of 0.130 and 0.171 compared to 0.161) and stronger XB for Cl^- (BSO values of 0.335 and 0.368 compared to 0.261) with high 3c-4e character (101% and 88%).

INTRINSIC XB STRENGTH AND COMPLEX BINDING ENERGIES

There is a tendency of considering the binding energy ΔE of XB complexes as a direct result of the intrinsic strength of XB. This simplification overlooks that, even in the structurally simplest XB complex, the magnitude of ΔE is determined by many factors rather than just the intrinsic strength of the XB. This also holds for dihalogens and interhalogens interacting with simple Lewis bases. The mutual polarization of the monomers leads in all cases to additional electronic effects, increasing the stability of the complex. Therefore, ΔE is not a simple reflection of the intrinsic strength of XB.

If one correlates the two XB complex properties BSO n(XA) and complex binding energy ΔE, one obtains the diagram shown in Figure 9. The scattering of data points suggests that there is no direct relationship between the two quantities. However, as indicated by the purple curve, which gives largely a linear relationship between n and ΔE based on the two reference molecules Cl_2···OF_2 (0.021) and FCl···OH_2 (0.134), three classes of XB complexes can be distinguished. The first class contains the phosphonium ion **106**, which has a covalent Cl−P bond, some Cl···C interactions, and a BSO(XB) value that is larger than suggested by ΔE (18.1 kcal/mol for Cl_2···PMe_3; however, 75.3 kcal/mol for Cl^-···$ClPMe_3^+$). In this class, one can also place systems **17**, **18**, or **107** with inverted 3c-4e character because they also have some (small) phosphonium character.

The second class contains complexes with strong 3c-4e bonding such as **7**, **13**−**16**, or **46**−**52**, which also have larger BSO values than ΔE values. Complex **19** belongs to this class but has a larger ΔE due to a HB between XY and Lewis base. Complexes such as **113**, **114**, or **115** have much larger binding energies as a result of the large polarizabilities of the monomers, which leads to stabilizing attractions between FX and the methyl groups of the phosphine that do not enhance the direct interactions between X and A but ΔE.

In the third class (to the left of the curve in Figure 9: larger ΔE values than expected from the BSO values), there are complexes with electrostatic and moderately covalent XB.

DOI: 10.1021/acs.inorgchem.6b02358
Inorg. Chem. 2017, 56, 488−502

Strong deviations from the expected ΔE can be observed for the perfluorinated halogen donors **195** and **196**, which are strongly polarizable and therefore have significantly higher binding energies ΔE. In this way, for each complex, additional stabilization effects can be quantitatively determined once a reasonable functional dependence has been established between n and ΔE with the help of a few reference systems.

One can extend this approach by comparing delocalization energies ΔE(del) with BSO values n (Figure 10). Scattering is stronger in this case because the magnitude of ΔE(del) depends on the orbital energies of lp(A) and $\sigma^{\star}$(XY) as well as their overlap. In the two previous sections, we have discussed the many effects determining orbital energies and overlap. On top of this, electrostatic interactions can increase the BSO value so that their magnitude becomes larger than expected from ΔE(del) (examples are **51** or **52**). By using ΔE(del) for analysis, one has to be aware that its calculation is based on the assumption of a specific Lewis structure, which in the case of nonclassical 3c-4e bonding leads to exaggerated delocalization energies. One can calculate with the perturbational molecular orbital approach 3c energies.[124] However, we have refrained from using this approach and have excluded complexes with strong 3c-4e bonding from the diagram in Figure 10 on which the analysis of the covalent contributions was based.

CONCLUSIONS AND OUTLOOK

The strength of the XB of 202 complexes has been determined for the first time quantitatively using local stretching force constants, which reflect local features of the curvature of the potential energy surface and can be directly related to measured or calculated frequencies.[86,89,90] The current investigation is put into perspective with regard to other quantum-chemical investigations of the recent years in Table 1. On the basis of this comparison, a solid basis for future studies on more sophisticated XB complexes is laid in the current work. Our work has led to the following conclusions.

1. On the basis of the calculated BSO values, one can distinguish weak ($n < 0.1$), normal ($0.1 \leq n \leq 0.3$), and strong ($n > 0.3$) XB. Complexes with n close to 0.5 benefit from nonclassical 3c-4e bonding. Complexes with $n > 0.5$ result from a transfer of the halogen cation X^+ from a polarized XY or XX to the halogen acceptor and the formation of an ion pair that itself is bonded by an inverted XB between the remaining halogen anion (as Lewis base) and the halogenated Lewis base as a new halogen donor. An example for such a X^+ transfer is $Cl_2\cdots PMe_3 \rightarrow Cl^-\cdots ClPMe_3$.

2. We have established 10 different electronic effects to analyze and explain the observed XB strength order of the 202 XB complexes.

3. The majority of the XB investigated has sizable covalent contributions. There is not a single XB with a strongly positive energy density in the bond region, which according to the Cremer−Kraka criteria would indicate dominant electrostatic bonding. Typically, the weak XB identified in this work possess energy densities close to zero and dominant electrostatic character.

4. Covalent contributions have been characterized by CT from lp(A) to $\sigma^{\star}$(XY) and by the delocalization energy ΔE(del) associated with this process. In all cases, at least some covalent character of XB could be observed, which underlines that XB is, in general, more covalent than either HB or pnicogen bonding.[83,97]

Table 1. Comparison of Quantum-Chemical Investigations of XB Complexes[a]

XB complexes	method	properties and topics	ref
IV (6)	DFT-r4	ESP	20
I (22)	MP2	ΔE, r, J_{coup}	30
II (76)	CCSD(T), microwave	ΔE, r, k_σ	32
II (15)	CCSD(T)	ΔE, ED, r, Θ	34
III (18)	MP2	ΔE, r, $\Delta\omega$, IE	37
II (69)	CCSD(T)	benchmark r, ΔE	38
II, III (55)	DFT-r4 BLW	ΔE, IE, ED	41
III (100)	MP2	ΔE, r, ESP	46
III (8)	MP2	ΔE, ESP, ED	54
II,III (28)	SAPT	ΔE, ED, Θ XB vs CB, PB	66, 67
I (15)	SAPT	ΔE, ED, Θ	69
III (11)	DFT-r2	ESP, ΔE, r, ρ	72
II (30)	DFT-r4	dipole, ΔE	74
I (7)	MP2	ΔE, r, ED, ρ, Θ	75
I (14)	MP2	ρ, XB vs HB	76
I (16)	MP2	ΔE, r, J_{coup}	83
III, IV (57)	DFT-r4, MP2	ESP, ΔE, r	123, 125
IV (12)	MP2	ESP, ΔE, r, Θ	130
II (7)	DFT-r4 BLW	ΔE, r, ESP, ED, $\Delta\omega$, Θ, XB vs HB, CB, PB	133
I, II, III, IV (202)	CCSD(T), DFT-r4	ΔE, r, ρ, ESP, ω^a, k^a, BSO	this work

[a]Groups I−IV according to Figure 1 and the number of XB complexes studied given in parentheses. XC functionals of DFT are classified according to their rung in "Jacobs's ladder" (r2, GGA; r4, hybrid XC). ESP = electrostatic potential, ΔE = binding energy, J_{coup} = NMR spin−spin coupling constants, ED = energy decomposition, ρ = electron density, r = geometric parameters, k_σ = intermolecular force constant from microwave spectroscopy, $\Delta\omega$ = frequency shifts, Θ = angular distortion, CB = comparison with chalcogen bonding, and PB = with pnicogen bonding.

5. It is remarkable that, besides the covalent contributions, the σ-hole,lp(A) interactions, as measured by the electrostatic potential V, are often decisive for the magnitude of the BSO because they directly influence the intrinsic bond strength. For example, the increasing intrinsic XB strength in the interactions of FCl, FBr, FI, and FAt with a Lewis base such as PMe_3 can be predicted in this way. However, it is a simplification to explain XB just by σ-hole interactions because covalent contributions to XB always have to be considered.

6. Unusual are the relatively strong XB between dihalogens/interhalogens and phosphines, especially if these are carrying an electron-withdrawing substituent such as Z = F, OH, Cl, CN, etc. In these cases, 3c-4e bonding is established leading to an interaction of the type Y···X···PR_2Z. The degree of 3c-4e XB is quantitatively determined by the ratio BSO(X···A)/BSO(Y···X). If the latter is close to 1.00, an ideal 3c-4e system is established. If it is larger than 1.00, then an inverted 3c-4e XB exists, with a stronger X−A interaction that in the extreme can lead to a new bond.

7. Relativistic effects both strengthen and weaken XB because of the s,p-orbital contraction for Br (small effect), I, and At. Orbital contraction increases somewhat the effective electronegativity, which causes a less steep decrease of the covalent contribution, as would be predicted by nonrelativistic orbital energies and the overlap with A. Second, they lead to a smaller σ hole (stronger shielding of the nucleus by orbital contraction)

DOI: 10.1021/acs.inorgchem.6b02358
Inorg. Chem. 2017, 56, 488−502

for the higher halogens, as expected on the basis of their atomic number. Compared to the nonrelativistic effects, the relativistic effects are too small to change the overall trends in covalent or electrostatic XB.

8. It is remarkable that, because of the formation of a supporting HB, the otherwise destabilizing OH group can substantially increase the intrinsic strength of XB. In the case of $FCl\cdots PH_2OH$, a nonclassical complex is formed with ideal 3c-4e bonding. We suggest exploiting the combination of HB and XB systematically to generate new polymers and other materials.

9. Halomethanes and halotetraganes are limited in establishing strong covalent contributions to XB. This is actually a result of the relatively low electronegativity of C (and the higher tetragenes) and the limited polarity of the C−X (Si−X, Ge−X, and Sn−X) bond. These limitations can be overcome by increasing the σ hole and polarizability of X, which is best accomplished by reverting to iodo-substituted carbon molecules. Essential is that the carbon framework is also highly polarizable, which is achieved if carbon molecules with multiple bonds are involved. This explains the stability of XB in connection with diiodoacetylene or diodopolyalkyne and their frequent use in polymer chemistry.[16,154−156]

10. We suggest as new materials the use of perfluorinated diiodobenzene, which has relatively strong XB with alkylamines and gains stability by its large polarizability. Iodocyanide should be too poisonous to use, iodophosphaethyne (I−C≡P) should only be stable at low temperatures, and diododizomethane (I_2CN_2) should be explosive, which limits the possibility of utilizing strong XB for systems with triple or multiple bonds. However, I-substituted derivatives of 1,3-dipolar molecules such as diazonium betaines (INNN and I_2CNN), nitrilium betaines (ICNO, ICNI, and $ICNCR_2$), or azomethines should provide possibilities for polymers if reacted with diamino perfluorinated polyalkenes or diaminopolyalkynes. 1,3-dipolar cycloadditions would lead to a very stable network of bonds in such polymers.

11. Apart from providing for the first time a quantitative order of intrinsic XB strengths, we have developed a new method for analyzing complex binding energies ΔE. This is based on two or three reference complexes that are used to establish a relationship between ΔE and BSO n. Any deviation from the reference line can be analyzed in terms of the electronic effects, causing the deviation. This makes it possible to quantify the energetic consequences of the latter and get a better understanding of how the interplay of different electronic effects leads to the actual complex binding energy. Similarly, one can analyze the delocalization energies ΔE(del), electron density $\rho(\mathbf{r}_b)$, or energy density $H(\mathbf{r}_b)$ by comparing them with the BSO values and using suitable reference values.

Finally, a caveat has to be made with regard to the σ-hole,lp(A) interactions because one might consider them to be a covalent contribution in the sense that the "lp(A) orbital directly donates charge to the σ-hole". However, covalent contributions always depend on both potential *and kinetic energy*. In this work, the energy density $H(\mathbf{r}_b)$ was used to determine the covalency of XB. It was found that $H(\mathbf{r})$ is not necessarily a minimum at the position of the σ hole, which indicates that analysis of the σ hole can provide some insight into the electrostatic but not the potential covalent character of XB. Additional covalent contributions, even if small, can change the intrinsic strength of XB.

■ ASSOCIATED CONTENT

Supporting Information

The Supporting Information is available free of charge on the ACS Publications website at DOI: 10.1021/acs.inorgchem.6b02358.

Binding energies ΔE, local stretching force constants k^a(XA), and bond distances r(XA) obtained at CCSD(T)/aug-cc-pVTZ and at ωB97X-D/aug-cc-pVTZ for selected complexes (Table S1 and Figures S1 and S2), a summary of energetic, geometric, and vibrational data for all complexes (Table S2), selected properties of the XB donors (Table S3) and acceptors (Table S4), bond distances and bond ratios of complexes of high 3c-4e character (Table S5), the corresponding BSO ratios (Table S6), lists of complexes (Tables S7−S10), a comparison between ΔE calculated at ωB97X-D/aug-cc-pVTZ geometries using ωB97X-D/aug-cc-pVTZ and CCSD(T)/aug-cc-pVTZ energies for all complexes (Figure S2), a schematic representation of all complexes with NBO charges (Figures S3−S5), a comparison of BSO n with the density ρ_b (Figure S6), and linear relationship between k^a(XA) and the calculated vertical IPs for 11 Lewis bases (Figure S7) (PDF)

■ AUTHOR INFORMATION

Corresponding Authors

*E-mail: ekraka@gmail.com.
*E-mail: dcremer@smu.edu.

ORCID

Elfi Kraka: 0000-0002-9658-5626
Dieter Cremer: 0000-0002-6213-5555

Notes

The authors declare no competing financial interest.

■ ACKNOWLEDGMENTS

This work was financially supported by National Science Foundation Grants CHE 1152357 and CHE 1464906. We thank SMU for providing computational resources. The authors acknowledge financial support by CAPES (Brazil; Fellowship Grant BEX 9534-13-0).

■ REFERENCES

(1) Cavallo, G.; Metrangolo, P.; Milani, R.; Pilati, T.; Priimagi, A.; Resnati, G.; Terraneo, G. The Halogen Bond. *Chem. Rev.* **2016**, *116*, 2478−2601.

(2) Pennington, W. T.; Hanks, T. W.; Arman, H. D. In *Halogen Bonding*; Metrangolo, P., Resnati, G., Eds.; Structure and Bonding; Springer: Berlin, 2008; Vol. *126*; pp 65−104.

(3) Beale, T. M.; Chudzinski, M. G.; Sarwar, M. G.; Taylor, M. S. Halogen bonding in solution: thermodynamics and applications. *Chem. Soc. Rev.* **2013**, *42*, 1667−1680.

(4) Wolters, L. P.; Schyman, P.; Pavan, M. J.; Jorgensen, W. L.; Bickelhaupt, F. M.; Kozuch, S. The many faces of halogen bonding: a review of theoretical models and methods. *WIREs Comput. Mol. Sci.* **2014**, *4*, 523−540.

(5) Gilday, L. C.; Robinson, S. W.; Barendt, T. A.; Langton, M. J.; Mullaney, B. R.; Beer, P. D. Halogen Bonding in Supramolecular Chemistry. *Chem. Rev.* **2015**, *115*, 7118−7195.

(6) Schindler, S.; Huber, S. M. In *Halogen Bonding II*; Metrangolo, P., Resnati, G., Eds.; Topics in Current Chemistry; Springer International Publishing: Berlin, 2015; Vol. *359*; pp 167−203.

DOI: 10.1021/acs.inorgchem.6b02358
Inorg. Chem. 2017, 56, 488−502

(7) Ho, P. In *Halogen Bonding I*; Metrangolo, P., Resnati, G., Eds.; Topics in Current Chemistry; Springer International Publishing: Berlin, 2015; Vol. *358*; pp 241−276.
(8) Jentzsch, A. V.; Matile, S. In *Halogen Bonding I*; Metrangolo, P., Resnati, G., Eds.; Topics in Current Chemistry; Springer International Publishing: Berlin, 2015; Vol. *358*; pp 205−239.
(9) Bauzá, T. J.; Mooibroek, T. J.; Frontera, A. The Bright Future of Unconventional σ/π-Hole Interactions. *ChemPhysChem* **2015**, *16*, 2496−2517.
(10) Kolar, M. H.; Hobza, P. Computer Modeling of Halogen Bonds and Other σ-Hole Interactions. *Chem. Rev.* **2016**, *116*, 5155−5187.
(11) Wang, H.; Wang, W.; Jin, W. J. σ-Hole Bond vs π-Hole Bond: A Comparison Based on Halogen Bond. *Chem. Rev.* **2016**, *116*, 5072−5104.
(12) Abate, A.; Saliba, M.; Hollman, D. J.; Stranks, S. D.; Wojciechowski, K.; Avolio, R.; Grancini, G.; Petrozza, A.; Snaith, H. J. Supramolecular Halogen Bond Passivation of Organic-Inorganic Halide Perovskite Solar Cells. *Nano Lett.* **2014**, *14*, 3247−3254.
(13) Aakeroy, C. B.; Spartz, C. L.; Dembowski, S.; Dwyre, S.; Desper, J. A systematic structural study of halogen bonding *versus* hydrogen bonding within competitive supramolecular systems. *IUCrJ* **2015**, *2*, 498−510.
(14) Aakeroy, C. B.; Wijethunga, T. K.; Desper, J.; Dakovic, M. Crystal Engineering with Iodoethynylnitrobenzenes: A Group of Highly Effective Halogen-Bond Donors. *Cryst. Growth Des.* **2015**, *15*, 3853−3861.
(15) Dumele, O.; Trapp, N.; Diederich, F. Halogen Bonding Molecular Capsules. *Angew. Chem., Int. Ed.* **2015**, *54*, 12339−12344.
(16) Berger, G.; Soubhye, J.; Meyer, F. Halogen bonding in polymer science: from crystal engineering to functional supramolecular polymers and materials. *Polym. Chem.* **2015**, *6*, 3559−3580.
(17) Dumele, O.; Wu, D.; Trapp, N.; Goroff, N.; Diederich, F. Halogen Bonding of (Iodoethynyl)benzene Derivatives in Solution. *Org. Lett.* **2014**, *16*, 4722−4725.
(18) Nagels, N.; Geboes, Y.; Pinter, B.; DeProft, F.; Herrebout, W. A. Tuning the Halogen/Hydrogen Bond Competition: A Spectroscopic and Conceptual DFT Study of Some Model Complexes Involving CHF2I. *Chem. - Eur. J.* **2014**, *20*, 8433−8443.
(19) Saito, M.; Tsuji, N.; Kobayashi, Y.; Takemoto, Y. Direct Dehydroxylative Coupling Reaction of Alcohols with Organosilanes through Si-X Bond Activation by Halogen Bonding. *Org. Lett.* **2015**, *17*, 3000−3003.
(20) Aakeroy, C. B.; Wijethunga, T. K.; Desper, J.; Moore, C. Halogen-Bond Preferences in Co-crystal Synthesis. *J. Chem. Crystallogr.* **2015**, *45*, 267−276.
(21) Kee, C. W.; Wong, M. W. In Silico Design of Halogen-Bonding-Based Organocatalyst for Diels-Alder Reaction, Claisen Rearrangement, and Cope-Type Hydroamination. *J. Org. Chem.* **2016**, *81*, 7459−7470.
(22) Kniep, F.; Jungbauer, S. H.; Zhang, Q.; Walter, S. M.; Schindler, S.; Schnapperelle, I.; Herdtweck, E.; Huber, S. M. Organocatalysis by Neutral Multidentate Halogen-Bond Donors. *Angew. Chem., Int. Ed.* **2013**, *52*, 7028−7032.
(23) Wilcken, R.; Zimmermann, M. O.; Lange, A.; Joerger, A. C.; Boeckler, F. M. Principles and Applications of Halogen Bonding in Medicinal Chemistry and Chemical Biology. *J. Med. Chem.* **2013**, *56*, 1363−1388.
(24) Alkorta, I.; Elguero, J.; Mo, O.; Yanez, M.; Del Bene, J. E. Using beryllium bonds to change halogen bonds from traditional to chlorine-shared to ion-pair bonds. *Phys. Chem. Chem. Phys.* **2015**, *17*, 2259−2267.
(25) Brea, O.; Mo, O.; Yanez, M.; Alkorta, I.; Elguero, J. Creating σ-Holes through the Formation of Beryllium Bonds. *Chem. - Eur. J.* **2015**, *21*, 12676−12682.
(26) Legon, A. C. Prereactive Complexes of Dihalogens XY with Lewis Bases B in the Gas Phase: A Systematic Case for the Halogen Analogue B···XY of the Hydrogen Bond B···HX. *Angew. Chem., Int. Ed.* **1999**, *38*, 2686−2714.
(27) Aragoni, M. C.; Arca, M.; Devillanova, M.; Garau, F. A.; Isaia, A.; Lippolis, F.; Mancini, A. The nature of the chemical bond in linear three-body systems: From I 3- to mixed chalcogen/halogen and trichalcogen moieties. *Bioinorg. Chem. Appl.* **2007**, *2007*, 1.
(28) Braida, B.; Hiberty, P. C. Application of the Valence Bond Mixing Configuration Diagrams to Hypervalency in Trihalide Anions: A Challenge to the Rundle-Pimentel Model. *J. Phys. Chem. A* **2008**, *112*, 13045−13052.
(29) Del Bene, J. E.; Alkorta, I.; Elguero, J. Do Traditional, Chlorine-shared, and Ion-pair Halogen Bonds Exist? An ab Initio Investigation of FCl:CNX Complexes. *J. Phys. Chem. A* **2010**, *114*, 12958−12962.
(30) Del Bene, J. E.; Alkorta, I.; Elguero, J. Do nitrogen bases form chlorine-shared and ion-pair halogen bonds? *Chem. Phys. Lett.* **2011**, *508*, 6−9.
(31) Donoso-Tauda, O.; Jaque, P.; Elguero, J.; Alkorta, I. Traditional and ion-pair halogen-bonded complexes between chlorine and bromine derivatives and a nitrogen-heterocyclic carbene. *J. Phys. Chem. A* **2014**, *118*, 9552−9560.
(32) Legon, A. C. A reduced radial potential energy function for the halogen bond and the hydrogen bond in complexes B···XY and B···HX, where X and Y are halogen atoms. *Phys. Chem. Chem. Phys.* **2014**, *16*, 12415−12421.
(33) Otero de la Roza, A.; Johnson, E. R.; DiLabio, G. A. Halogen Bonding from Dispersion-Corrected Density-Functional Theory: The Role of Delocalization Error. *J. Chem. Theory Comput.* **2014**, *10*, 5436−5447.
(34) Hill, J. G.; Hu, X. Theoretical Insights into the Nature of Halogen Bonding in Prereactive Complexes. *Chem. - Eur. J.* **2013**, *19*, 3620−3628.
(35) Karpfen, A. *Halogen Bonding* **2008**, *126*, 1−15.
(36) Wolters, L. P.; Bickelhaupt, F. M. Halogen Bonding versus Hydrogen Bonding: A Molecular Orbital Perspective. *ChemistryOpen* **2012**, *1*, 96−105.
(37) Pinter, B.; Nagels, N.; Herrebout, W. A.; DeProft, F. Halogen Bonding from a Hard and Soft Acids and Bases Perspective: Investigation by Using Density Functional Theory Reactivity Indices. *Chem. - Eur. J.* **2013**, *19*, 519−530.
(38) Kozuch, S.; Martin, J. M. L. Halogen Bonds: Benchmarks and Theoretical Analysis. *J. Chem. Theory Comput.* **2013**, *9*, 1918−1931.
(39) Forni, A.; Pieraccini, S.; Rendine, S.; Sironi, M. Halogen bonds with benzene: An assessment of DFT functionals. *J. Comput. Chem.* **2014**, *35*, 386−394.
(40) Tognetti, V.; Joubert, L. Electron density Laplacian and halogen bonds. *Theor. Chem. Acc.* **2015**, *134*.10.1007/s00214-015-1685-8
(41) Wang, C.; Danovich, D.; Mo, Y.; Shaik, S. On The Nature of the Halogen Bond. *J. Chem. Theory Comput.* **2014**, *10*, 3726−3737.
(42) George, J.; Deringer, V. L.; Dronskowski, R. Cooperativity of Halogen, Chalcogen, and Pnictogen Bonds in Infinite Molecular Chains by Electronic Structure Theory. *J. Phys. Chem. A* **2014**, *118*, 3193−3200.
(43) Parker, A. J.; Stewart, J.; Donald, K. J.; Parish, C. A. Halogen Bonding in DNA Base Pairs. *J. Am. Chem. Soc.* **2012**, *134*, 5165−5172.
(44) Palusiak, M. On the nature of halogen bond - The Kohn-Sham molecular orbital approach. *J. Mol. Struct.: THEOCHEM* **2010**, *945*, 89−92.
(45) Del Bene, J. E.; Alkorta, I.; Elguero, J. Influence of Substituent Effects on the Formation of P···Cl Pnicogen Bonds or Halogen Bonds. *J. Phys. Chem. A* **2014**, *118*, 2360−2366.
(46) Tawfik, M.; Donald, K. J. Halogen Bonding: Unifying Perspectives on Organic and Inorganic Cases. *J. Phys. Chem. A* **2014**, *118*, 10090−10100.
(47) Bartashevich, E. V.; Tsirelson, V. G. Interplay between non-covalent interactions in complexes and crystals with halogen bonds. *Russ. Chem. Rev.* **2014**, *83*, 1181.
(48) Duarte, D. J. R.; Peruchena, N. M.; Alkorta, I. Double Hole-Lump Interaction between Halogen Atoms. *J. Phys. Chem. A* **2015**, *119*, 3746−3752.

DOI: 10.1021/acs.inorgchem.6b02358
Inorg. Chem. 2017, 56, 488−502

(49) Jahromi, H. J.; Eskandari, K.; Alizadeh, A. Comparison of halogen bonds in M-X···N contacts (M = C, Si, Ge and X = Cl, Br). *J. Mol. Model.* **2015**, *21*.10.1007/s00894-015-2660-y
(50) Lo, R.; Ganguly, B. Revealing halogen bonding interactions with anomeric systems: An ab initio quantum chemical studies. *J. Mol. Graphics Modell.* **2015**, *55*, 123−133.
(51) Sladek, V.; Skorna, P.; Poliak, P.; Lukes, V. The ab initio study of halogen and hydrogen σN-bonded para-substituted pyridine···(X2/XY/HX) complexes. *Chem. Phys. Lett.* **2015**, *619*, 7−13.
(52) Nepal, B.; Scheiner, S. Long-range behavior of noncovalent bonds. Neutral and charged H-bonds, pnicogen, chalcogen, and halogen bonds. *Chem. Phys.* **2015**, *456*, 34−40.
(53) Huber, S. M.; Jimenez-Izal, E.; Ugalde, J. M.; Infante, I. Unexpected trends in halogen-bond based noncovalent adducts. *Chem. Commun.* **2012**, *48*, 7708−7710.
(54) Alkorta, I.; Blanco, F.; Solimannejad, M.; Elguero, J. Competition of Hydrogen Bonds and Halogen Bonds in Complexes of Hypohalous Acids with Nitrogenated Bases. *J. Phys. Chem. A* **2008**, *112*, 10856−10863.
(55) Grant Hill, J. The halogen bond in thiirane···ClF: an example of a Mulliken inner complex. *Phys. Chem. Chem. Phys.* **2014**, *16*, 19137−19140.
(56) Grant Hill, J.; Legon, A. C. On the directionality and non-linearity of halogen and hydrogen bonds. *Phys. Chem. Chem. Phys.* **2015**, *17*, 858−867.
(57) Jeffrey, G. *An Introduction to Hydrogen Bonding*; Oxford University Press: New York, 1997.
(58) Jeffrey, G.; Saenger, W. *Hydrogen Bonding in Biological Structures*; Springer-Verlag: Berlin, 1991.
(59) Scheiner, S. *Hydrogen bonding: A theoretical perspective*; Oxford University Press: New York, 1997.
(60) Pihko, P. E. *Hydrogen Bonding in Organic Synthesis*; Wiley: New York, 2009.
(61) Grabowski, E. *Hydrogen Bonding—New Insights (Challenges and Advances in Computational Chemistry and Physics)*; Springer: New York, 2006.
(62) Gilli, G.; Gilli, P. *The Nature of the Hydrogen Bond*; IUCr Monographs on Crystallography 23;Oxford University Press: New York, 2009.
(63) Cavallo, G.; Metrangolo, P.; Pilati, T.; Resnati, G.; Sansotera, M.; Terraneo, G. Halogen bonding: a general route in anion recognition and coordination. *Chem. Soc. Rev.* **2010**, *39*, 3772−3783.
(64) Metrangolo, P.; Meyer, F.; Pilati, T.; Resnati, G.; Terraneo, G. Halogen Bonding in Supramolecular Chemistry. *Angew. Chem., Int. Ed.* **2008**, *47*, 6114−6127.
(65) Adhikari, U.; Scheiner, S. Substituent Effects on Cl···N, S···N, and P···N Noncovalent Bonds. *J. Phys. Chem. A* **2012**, *116*, 3487−3497.
(66) Scheiner, S. Detailed comparison of the pnicogen bond with chalcogen, halogen, and hydrogen bonds. *Int. J. Quantum Chem.* **2013**, *113*, 1609−1620.
(67) Riley, K. E.; Murray, J. S.; Fanfrlík, J.; Rezác, J.; Solá, R. J.; Concha, M. C.; Ramos, F. M.; Politzer, P. Halogen bond tunability II: the varying roles of electrostatic and dispersion contributions to attraction in halogen bonds. *J. Mol. Model.* **2013**, *19*, 4651−4659.
(68) Stone, A. J. Are Halogen Bonded Structures Electrostatically Driven? *J. Am. Chem. Soc.* **2013**, *135*, 7005−7009.
(69) Sedlak, R.; Kolár, M. H.; Hobza, P. Polar Flattening and the Strength of Halogen Bonding. *J. Chem. Theory Comput.* **2015**, *11*, 4727−4732.
(70) Zierkiewicz, W.; Bienko, D. C.; Michalska, D.; Zeegers-Huyskens, T. Theoretical investigation of the halogen bonded complexes between carbonyl bases and molecular chlorine. *J. Comput. Chem.* **2015**, *36*, 821−832.
(71) Dyduch, K.; Mitoraj, M. P.; Michalak, A. ETS-NOCV description of σ-hole bonding. *J. Mol. Model.* **2013**, *19*, 2747−2758.
(72) Mitoraj, M. P.; Michalak, A. Theoretical description of halogen bonding - an insight based on the natural orbitals for chemical valence combined with the extended-transition-state method (ETS-NOCV). *J. Mol. Model.* **2013**, *19*, 4681−4688.
(73) Bartashevich, E. V.; Tsirelson, V. G. Atomic dipole polarization in charge-transfer complexes with halogen bonding. *Phys. Chem. Chem. Phys.* **2013**, *15*, 2530−2538.
(74) Duarte, D.; Sosa, G.; Peruchena, N. Nature of halogen bonding. A study based on the topological analysis of the Laplacian of the electron charge density and an energy decomposition analysis. *J. Mol. Model.* **2013**, *19*, 2035−2041.
(75) Angelina, E. L.; Duarte, D. R.; Peruchena, N. M. Is the decrease of the total electron energy density a covalence indicator in hydrogen and halogen bonds? *J. Mol. Model.* **2013**, *19*, 2097−2106.
(76) Grabowski, S. J. Non-covalent interactions - QTAIM and NBO analysis. *J. Mol. Model.* **2013**, *19*, 4713−4721.
(77) Duarte, D., Angelina, E. L., Peruchena, N. Physical meaning of the QTAIM topological parameters in hydrogen bonding. *J. Mol. Model.* **2014**, *20*.10.1007/s00894-014-2510-3
(78) Shahi, A.; Arunan, E. Hydrogen bonding, halogen bonding and lithium bonding: an atoms in molecules and natural bond orbital perspective towards conservation of total bond order, inter- and intra-molecular bonding. *Phys. Chem. Chem. Phys.* **2014**, *16*, 22935−22952.
(79) Kaur, D.; Kaur, R.; Shiekh, B. Effects of substituents and charge on the RCHO···X-Y X= Cl, Br, I; Y:Ä†-CF3, -CF2H, -CFH2, -CN, -CCH, -CCCN; R:†-OH, -OCH3, -NH2, -O- halogen-bonded complexes. *Struct. Chem.* **2016**, *27*, 961.
(80) Joy, J.; Jemmis, E. D.; Vidya, K. Negative hyperconjugation and red-, blue- or zero-shift in X-Z···Y complexes. *Faraday Discuss.* **2015**, *177*, 33−50.
(81) Joy, J.; Jose, A.; Jemmis, E. D. Continuum in the X-Z-Y weak bonds: Z= main group elements. *J. Comput. Chem.* **2016**, *37*, 270−279.
(82) Alkorta, I.; Elguero, J.; Del Bene, J. E. Characterizing Traditional and Chlorine-Shared Halogen Bonds in Complexes of Phosphine Derivatives with ClF and Cl_2. *J. Phys. Chem. A* **2014**, *118*, 4222−4231.
(83) Freindorf, M.; Kraka, E.; Cremer, D. A Comprehensive Analysis of Hydrogen Bond Interactions Based on Local Vibrational Modes. *Int. J. Quantum Chem.* **2012**, *112*, 3174−3187.
(84) Kraka, E.; Setiawan, D.; Cremer, D. Reevaluation of the Bond Length - Bond Strength Rule: The Stronger Bond is not always the Shorter Bond. *J. Comput. Chem.* **2016**, *37*, 130−142.
(85) Konkoli, Z.; Cremer, D. A New Way of Analyzing Vibrational Spectra I. Derivation of Adiabatic Internal Modes. *Int. J. Quantum Chem.* **1998**, *67*, 1−9.
(86) Cremer, D.; Larsson, J. A.; Kraka, E. In *Theoretical and Computational Chemistry, Vol. 5, Theoretical Organic Chemistry*; Parkanyi, C., Ed.; Elsevier: Amsterdam, The Netherlands, 1998; pp 259−327.
(87) Zou, W.; Kalescky, R.; Kraka, E.; Cremer, D. Relating Normal Vibrational Modes To Local Vibrational Modes With The Help of an Adiabatic Connection Scheme. *J. Chem. Phys.* **2012**, *137*, 084114.
(88) Zou, W.; Cremer, D. Properties of Local Vibrational Modes: The Infrared Intensity. *Theor. Chem. Acc.* **2014**, *133*, 1451-1−1451-15.
(89) Kalescky, R.; Zou, W.; Kraka, E.; Cremer, D. Local Vibrational Modes of the Water Dimer - Comparison of Theory and Experiment. *Chem. Phys. Lett.* **2012**, *554*, 243−247.
(90) Kalescky, R.; Kraka, E.; Cremer, D. Local Vibrational Modes of the Formic Acid Dimer - The Strength of the Double Hydrogen Bond. *Mol. Phys.* **2013**, *111*, 1497−1510.
(91) Kalescky, R.; Kraka, E.; Cremer, D. Identification of the Strongest Bonds in Chemistry. *J. Phys. Chem. A* **2013**, *117*, 8981−8995.
(92) Kalescky, R.; Zou, W.; Kraka, E.; Cremer, D. Vibrational properties of the Isotopomers of the Water Dimer Derived from Experiment and Computations. *Aust. J. Chem.* **2014**, *67*, 426−434.
(93) Kraka, E.; Freindorf, M.; Cremer, D. Chiral Discrimination by Vibrational Spectroscopy Utilizing Local Modes. *Chirality* **2013**, *25*, 185−196.
(94) Zhang, X.; Dai, H.; Yan, H.; Zou, H. Y. W.; Cremer, D. B-H ···π Interaction: A New Type of Nonclassical Hydrogen Bonding. *J. Am. Chem. Soc.* **2016**, *138*, 4334−4337.

DOI: 10.1021/acs.inorgchem.6b02358
Inorg. Chem. 2017, 56, 488−502

(95) Zou, W.; Kalescky, R.; Kraka, E.; Cremer, D. Relating normal vibrational modes to local vibrational modes benzene and naphthalene. *J. Chem. Phys.* **2012**, *137*, 084114-1−084114-13.
(96) Zou, W.; Cremer, D. C_2 in a Box: Determining its Intrinsic Bond Strength for the $X^1\Sigma_g^+$ Ground State. *Chem. - Eur. J.* **2016**, *22*, 4087−4089.
(97) Setiawan, D.; Kraka, E.; Cremer, D. Strength of the Pnicogen Bond in Complexes Involving Group Va Elements N, P, and As. *J. Phys. Chem. A* **2015**, *119*, 1642−1656.
(98) Setiawan, D.; Kraka, E.; Cremer, D. Description of pnicogen bonding with the help of vibrational spectroscopy - The missing link between theory and experiment. *Chem. Phys. Lett.* **2014**, *614*, 136−142.
(99) Raghavachari, K.; Trucks, G. W.; Pople, J. A.; Head-Gordon, M. *Chem. Phys. Lett.* **1989**, *157*, 479−483.
(100) Woon, D.; Dunning, T. J. Gaussian Basis Sets for Use in Correlated Molecular Calculations. IV. Calculation of Static Electrical Response Properties. *J. Chem. Phys.* **1994**, *100*, 2975−2988.
(101) Dunning, T. Gaussian Basis Sets for Use in Correlated Molecular Calculations. I. The Atoms Boron Through Neon and Hydrogen. *J. Chem. Phys.* **1989**, *90*, 1007−1023.
(102) Woon, D.; Dunning, T. Gaussian Basis Sets for Use in Correlated Molecular Calculations. III. The Atoms Aluminum Through Argon. *J. Chem. Phys.* **1993**, *98*, 1358−1371.
(103) Peterson, K. A.; Figgen, D.; Goll, E.; Stoll, H.; Dolg, M. Systematically convergent basis sets with relativistic pseudopotentials. II. Small-core pseudopotentials and correlation consistent basis sets for the post-d group 16−18 elements. *J. Chem. Phys.* **2003**, *119*, 11113−11123.
(104) Grafenstein, J.; Cremer, D. Efficient DFT Integrations by Locally Augmented Radial Grids. *J. Chem. Phys.* **2007**, *127*, 164113.
(105) Chai, J. D.; Head-Gordon, M. Long-range Corrected Hybrid Density Functionals with Damped Atom-atom Dispersion Corrections. *Phys. Chem. Chem. Phys.* **2008**, *10*, 6615−6620.
(106) Chai, J. D.; Head-Gordon, M. Systematic Optimization of Long-range Corrected Hybrid Density Functionals. *J. Chem. Phys.* **2008**, *128*, 084106.
(107) Becke, A. D. Density-Functional Thermochemistry. III. The Role of Exact Exchange. *J. Chem. Phys.* **1993**, *98*, 5648−5652.
(108) Stephens, P. J.; Devlin, F. J.; Chabalowski, C. F.; Frisch, M. J. Ab Initio Calculation of Vibrational Absorption and Circular Dichroism Spectra Using Density Functional Force Fields. *J. Phys. Chem.* **1994**, *98*, 11623−11627.
(109) Perdew, J. P.; Burke, K.; Ernzerhof, M. Generalized Gradient Approximation Made Simple. *Phys. Rev. Lett.* **1996**, *77*, 3865−3869.
(110) Adamo, C.; Barone, V. Toward reliable density functional methods without adjustable parameters: The PBE0 model. *J. Chem. Phys.* **1999**, *110*, 6158−6169.
(111) Zhao, Y.; Truhlar, D. G. The M06 suite of density functionals for main group thermochemistry, thermochemical kinetics, noncovalent interactions, excited states, and transition elements: two new functionals and systematic testing of four M06-class functionals and 12 other functionals. *Theor. Chem. Acc.* **2008**, *120*, 215−241.
(112) Wilson, E. B.; Decius, J. C.; Cross, P. C. *Molecular Vibrations. The Theory of Infrared and Raman Vibrational Spectra*; McGraw-Hill: New York, 1955.
(113) Mayer, I. Charge, Bond Order an Valence in the Ab Initio Theory. *Chem. Phys. Lett.* **1983**, *97*, 270−274.
(114) Mayer, I. Bond orders and valences from ab initio wave functions. *Int. J. Quantum Chem.* **1986**, *29*, 477−483.
(115) Kraka, E.; Larsson, J. A.; Cremer, D. *Generalization of the Badger Rule Based on the Use of Adiabatic Vibrational Modes in Vibrational Modes in Computational IR Spectroscopy*; Wiley, New York, 2010; pp 105−149.
(116) Boys, S.; Bernardi, F. The Calculation of Small Molecular Interactions by The Differences of Separate Total Energies. Some Procedures with Reduced Errors. *Mol. Phys.* **1970**, *19*, 553−566.
(117) Riplinger, C.; Neese, F. An efficient and near linear scaling pair natural orbital based local coupled cluster method. *J. Chem. Phys.* **2013**, *138*, 034106-1−034106-18.
(118) Riplinger, C.; Sandhoefer, B.; Hansen, A.; Neese, F. Natural triple excitations in local coupled cluster calculations with pair natural orbitals. *J. Chem. Phys.* **2013**, *139*, 134101-1−134101-13.
(119) Weigend, F.; Ahlrichs, R. Balanced basis sets of split valence, triple zeta valence and quadruple zeta valence quality for H to Rn: Design and assessment of accuracy. *Phys. Chem. Chem. Phys.* **2005**, *7*, 3297−3305.
(120) Peterson, K. A.; Figgen, D.; Goll, E.; Stoll, H.; Dolg, M. Systematically convergent basis sets with relativistic pseudopotentials. II. Small-core pseudopotentials and correlation consistent basis sets for the post-d group 16−18 elements. *J. Chem. Phys.* **2003**, *119*, 11113−11123.
(121) Cremer, D.; Kraka, E. A Description of the Chemical Bond in Terms of Local Properties of Electron Density and Energy. *Croatica Chemica Acta* **1984**, *57*, 1259−1281.
(122) Cremer, D.; Kraka, E. Chemical Bonds without Bonding Electron Density - Does the Difference Electron Density Analysis Suffice for a Description of the Chemical Bond? *Angew. Chem., Int. Ed. Engl.* **1984**, *23*, 627−628.
(123) Kraka, E.; Cremer, D. In *Theoretical Models of Chemical Bonding. The Concept of the Chemical Bond,*; Maksic, Z., Ed.; Springer Verlag: Heidelberg, Germany, 1990; Vol. 2; pp 453−542.
(124) Weinhold, F.; Landis, C. R. *Valency and Bonding: A Natural Bond Orbital Donor−Acceptor Perspective*; University Press: Cambridge, U.K., 2003.
(125) Politzer, P.; Murray, J. S.; Clark, T. In *Halogen Bonding I: Impact on Materials Chemistry and Life Sciences*; Metrangolo, P., Resnati, G., Eds.; Springer International Publishing: Berlin, 2015; pp 19−42.
(126) Clark, T.; Hennemann, M.; Murray, J.; Politzer, P. Halogen bonding: the σ-hole. *J. Mol. Model.* **2007**, *13*, 291−296.
(127) Politzer, P.; Murray, J.; Concha, M. Halogen bonding and the design of new materials: organic bromides, chlorides and perhaps even fluorides as donors. *J. Mol. Model.* **2007**, *13*, 643−650.
(128) Politzer, P.; Murray, J. S.; Clark, T. Halogen bonding: an electrostatically-driven highly directional noncovalent interaction. *Phys. Chem. Chem. Phys.* **2010**, *12*, 7748−7757.
(129) Kraka, E.; Zou, W.; Filatov, M.; Grafenstein, J.; Izotov, D.; Gauss, J.; He, Y.; Wu, A.; Konkoli, Z.; Polo, V.; et al. *COLOGNE2016*; 2014; see http://www.smu.edu/catco.
(130) Stanton, J. F.; Gauss, J.; Harding, M. E.; Szalay, P. G.; et al. *CFOUR, A Quantum Chemical Program Package*; 2010; see http://www.cfour.de.
(131) Neese, F. The ORCA program system. *WIREs: Comp. Mol. Sci.* **2012**, *2*, 73−78.
(132) Keith, T. TK Gristmill Software: Overland Park, KS, 2011; aim.tkgristmill.com.
(133) Frisch, M. J.; Trucks, G. W.; Schlegel, H. B.; Scuseria, G. E.; Robb, M. A.; Cheeseman, J. R.; Scalmani, G.; Barone, V.; Mennucci, B.; Petersson, G. A.; et al. *Gaussian 09*, revision A.1; Gaussian Inc.: Wallingford, CT, 2010.
(134) Riley, K.; Murray, J.; Fanfrlík, J.; Rezác, J.; Solá, R.; Concha, M.; Ramos, F.; Politzer, P. Halogen bond tunability I: the effects of aromatic fluorine substitution on the strengths of halogen-bonding interactions involving chlorine, bromine, and iodine. *J. Mol. Model.* **2011**, *17*, 3309−3318.
(135) Politzer, P.; Murray, J. S. Halogen bonding and beyond: factors influencing the nature of CN-R and SiN-R complexes with F-Cl and Cl2. *Theor. Chem. Acc.* **2012**, *131*.10.1007/s00214-012-1114-1
(136) Kolar, M.; Hostas, J.; Hobza, P. The strength and directionality of a halogen bond are co-determined by the magnitude and size of the σ-hole. *Phys. Chem. Chem. Phys.* **2014**, *16*, 9987−9996.
(137) Wang, C.; Guan, L.; Danovich, D.; Shaik, S.; Mo, Y. The origins of the directionality of noncovalent intermolecular interactions. *J. Comput. Chem.* **2016**, *37*, 34−45.

DOI: 10.1021/acs.inorgchem.6b02358
Inorg. Chem. 2017, 56, 488−502

(138) Dyall, K. G., Fægri, K. *Introduction to Relativistic Quantum Chemistry*; Oxford University Press: Oxford, U.K., 2007.
(139) Rundle, R. E. Electron Deficient Compounds. II. Relative Energies of "Half-Bonds. *J. Chem. Phys.* **1949**, *17*, 671−675.
(140) Pimentel, G. C. The Bonding of Trihalide and Bifluoride Ions by the Molecular Orbital Method. *J. Chem. Phys.* **1951**, *19*, 446−448.
(141) Porterfield, W. W. *Inorganic Chemistry, A Unified Approach*; Academic Press: San Diego, 1993.
(142) Greenwood, N. N.; Earnshaw, A. *Chemistry of the Elements*; Butterworth-Heinemann: Oxford, U.K., 1997.
(143) Riley, K. E.; Hobza, P. Investigations into the Nature of Halogen Bonding Including Symmetry Adapted Perturbation Theory Analyses. *J. Chem. Theory Comput.* **2008**, *4*, 232−242.
(144) Filatov, M.; Zou, W.; Cremer, D. Spin-orbit coupling calculations with the two-component normalized elimination of the small component method. *J. Chem. Phys.* **2013**, *139*, 014106-1−014106-8.
(145) Marian, C. M. Spin-orbit coupling and intersystem crossing in molecules. *WIREs Comput. Mol. Sci.* **2012**, *2*, 187−203.
(146) Fedorov, D. G.; Koseki, S.; Schmidt, M. W.; Gordon, M. S. Spin-orbit coupling in molecules: Chemistry beyond the adiabatic approximation. *Int. Rev. Phys. Chem.* **2003**, *22*, 551−592.
(147) Clark, T.; Politzer, P.; Murray, J. S. Correct electrostatic treatment of noncovalent interactions: the importance of polarization. *WIRES Comp. Mol. Sci.* **2015**, *5*, 169−177.
(148) Politzer, P.; Murray, J. S.; Clark, T. Mathematical modeling and Physical Reality in Non-covalent Interactions. *J. Mol. Model.* **2015**, *21*, 52−61.
(149) Politzer, P.; Murray, J. S.; Clark, T. σ-Hole Bonding: A Physical Interpretation. *Top. Curr. Chem.* **2014**, *358*, 19−42.
(150) Dominikowska, J.; Jablonski, M.; Palusiak, M. Feynman force components: basis for a solution of the covalent vs. ionic dilemma. *Phys. Chem. Chem. Phys.* **2016**, *18*, 25022−25026.
(151) Metrangolo, P.; Resnati, G. Halogen Bonding: A Paradigm in Supramolecular Chemistry. *Chem. - Eur. J.* **2001**, *7*, 2511−2519.
(152) Cincic, D.; Friscic, T.; Jones, W. Isostructural Materials Achieved by Using Structurally Equivalent Donors and Acceptors in Halogen-Bonded Cocrystals. *Chem. - Eur. J.* **2008**, *14*, 747−753.
(153) Metrangolo, P.; Resnati, G.; Pilati, T.; Biella, S. In *Halogen Bonding: Fundamentals and Applications*; Metrangolo, P., Resnati, G., Eds.; Springer: Berlin, 2008; pp 105−136.
(154) Perkins, C.; Libri, S.; Adams, H.; Brammer, L. Diiodoacetylene: compact, strong ditopic halogen bond donor. *CrystEngComm* **2012**, *14*, 3033−3038.
(155) Luo, L.; Wilhelm, C.; Sun, A.; Grey, C. P.; Lauher, J. W.; Goroff, N. S. Poly(diiododiacetylene): Preparation, Isolation, and Full Characterization of a Very Simple Poly(diacetylene). *J. Am. Chem. Soc.* **2008**, *130*, 7702−7709.
(156) Goroff, N. S.; Curtis, S. M.; Webb, J. A.; Fowler, F. W.; Lauher, J. W. Designed Cocrystals Based on the Pyridine-Iodoalkyne Halogen Bond. *Org. Lett.* **2005**, *7*, 1891−1893.

DOI: 10.1021/acs.inorgchem.6b02358
Inorg. Chem. 2017, 56, 488−502